Available online at BCREC website: https://bcrec.id

Bulletin of Chemical Reaction Engineering & Catalysis, 15 (1) 2020, 1-34

Review Article

A Review Paper on Heterogeneous Fenton Catalyst: Types of Preparation, Modification Techniques, Factors Affecting the Synthesis, Characterization, and Application in the Wastewater Treatment

Vijyendra Kumar, Titikshya Mohapatra, Sandeep Dharmadhikari, Prabir Ghosh*

Department of Chemical Engineering, National Institute of Technology Raipur, 492010 India

Received: 1st May 2019; Revised: 20th August 2019; Accepted: 23rd August 2019;
Available online: 28th February 2020; Published regularly: April 2020

Abstract

This comprehensive review focuses on the different factors, modification in the synthesis method, characterization and application of heterogeneous catalyst in the wastewater treatment based on the Fenton process. The present review highlights the different catalyst preparation methods like wet impregnation method, hydrothermal method, sol-gel method, precipitation method and their application to treat different recalcitrant organic chemicals. Major heterogeneous catalyst synthesis methods were discussed with their excellent workability. The importance of modification through physical and chemical method was also reported. Different catalyst, pollutants and optimum parametric conditions available in the literature along with some relevant studies are summarized. The effect of factors like pH, calcination and some other modifiers on the synthesis and their efficiency in the wastewater treatment has been described. The important characterization of synthesized catalysts explaining their working efficiency has also been discussed. In the final section, the application of heterogeneous catalyst synthesized by different methods in the wastewater/effluent treatment has been investigated. The main aim of this review is to find out the influence of process parameters and catalytic method on degradation/decolorization of organic compounds present in industrial or synthetic wastewater.

Keywords: Catalytic Method; Fenton Process; Synthetic and Industrial Wastewater; Influence of Process Parameter; Modification of Catalyst Synthesis

How to Cite: Kumar, V., Mohapatra, T., Dharmadhikari, S., Ghosh, P. (2020). A Review Paper on Heterogeneous Fenton Catalyst: Types of Preparation, Modification Techniques, Factors Affecting the Synthesis, Characterization, and Application in the Wastewater Treatment. *Bulletin of Chemical Reaction Engineering & Catalysis*, 15(1), 1-34 (doi:10.9767/bcrec.15.1.4374.1-34)

Permalink/DOI: https://doi.org/10.9767/bcrec.15.1.4374.1-34

1. Introduction

Many researchers are working on the treatment of wastewater generated from different industries like printing, dye [1], plastic, paint [2], textile [3], food, leather [4], petroleum [5], paper [6], cosmetics [7], distilleries [8], steel, rice mill, sugar [9], fertilizers, pharmaceutical [10-13], sewage, oil extraction and refineries *etc.* [14-20]. These industries produce a huge amount of wastewater containing harmful organic compound that affects the environment directly or indirectly [21]. For instance, direct disposal of phenol and their derivatives into environment create serious issues for the living organism [22-27]. In the same way, dyes are also intolerable and unacceptable due to poisonous and their re-

* Corresponding Author.
E-mail: prbairg.che@nitrr.ac.in (P. Ghosh);
Tel.: +91 7773892359

fractory nature [28-30]. For the treatment of generated wastewater, various conventional and non-conventional methods like coagulation method [31], biological method [32], ion exchange method have been used, but among these methods, advanced oxidation technology (AOTs) is very effective comparatively [16,33]. During advanced oxidation reaction process, an oxidizing agent (•OH radical) reacts with pollutant and degrades almost all the harmful recalcitrant compounds into CO_2, H_2O, and inorganic salts [34]. Hydroxyl radical (•OH) is one of the strongest oxidizing oxidants (E^0 =2.73 V). Hydroxyl radical generation is the basic principle of AOPs, produced by using hydrogen peroxide, UV-catalyst, O_3, etc. and it mineralizes almost all organic chemicals [35].

The role of heterogeneous catalyst, preparation method, and process parameters are very important in the advanced oxidation processes. The applicability of catalysts has vast areas: chemical engineering, material science, surface science, biochemistry, organic chemistry and inorganic chemistry [36]. Some examples of heterogeneous catalyst and pollutants are Fe-SBA-15/H_2O_2 and Rhodamine B [28], FeO_x,SiO_2,TiO_2/Ti/H_2O_2 and phenol [22], FeZSM-5 and Reactive Red 120 [29], Fe^{3+}/Cu^{2+}-grafted ZnO [37], copper loaded bentonite and Yellow FCF [38], Cu-Zeolites and 2-(methylmercapto)-benzothiazole [39], Fe/clinoptilolite zeolite and phenol [23], Cu-modified alkalinized g-C_3N_4 [40], CuO/Fe_2O_3/SBA-15 and N, N-diethyl-p-phenyl diamine degradation [41], Fe_2O_3/ACF and of acid red B [42], Fe/OMC and 4-chlorophenol [24], GO-Fe_2O_3 [43], HPW-Fe-Bent and methyl orange[44], Fe/meso-Al_2O_3 and phenol [45], Fe(III)-SiO_2 and polyacrylamide [46], Fe(III)-HY[47], Fe-doped TiO_2 and carboxylic acids [48], $Cs_xH_{3-x}PW_{12}O_{40}$ [49], CuFeZSM-5 and Rhodamine 6G [50], Bi-doped goethite–hematite and actual pesticide [51], Ag_2O-ZnO [52], Schwertmannite and phenol [26], Fe-

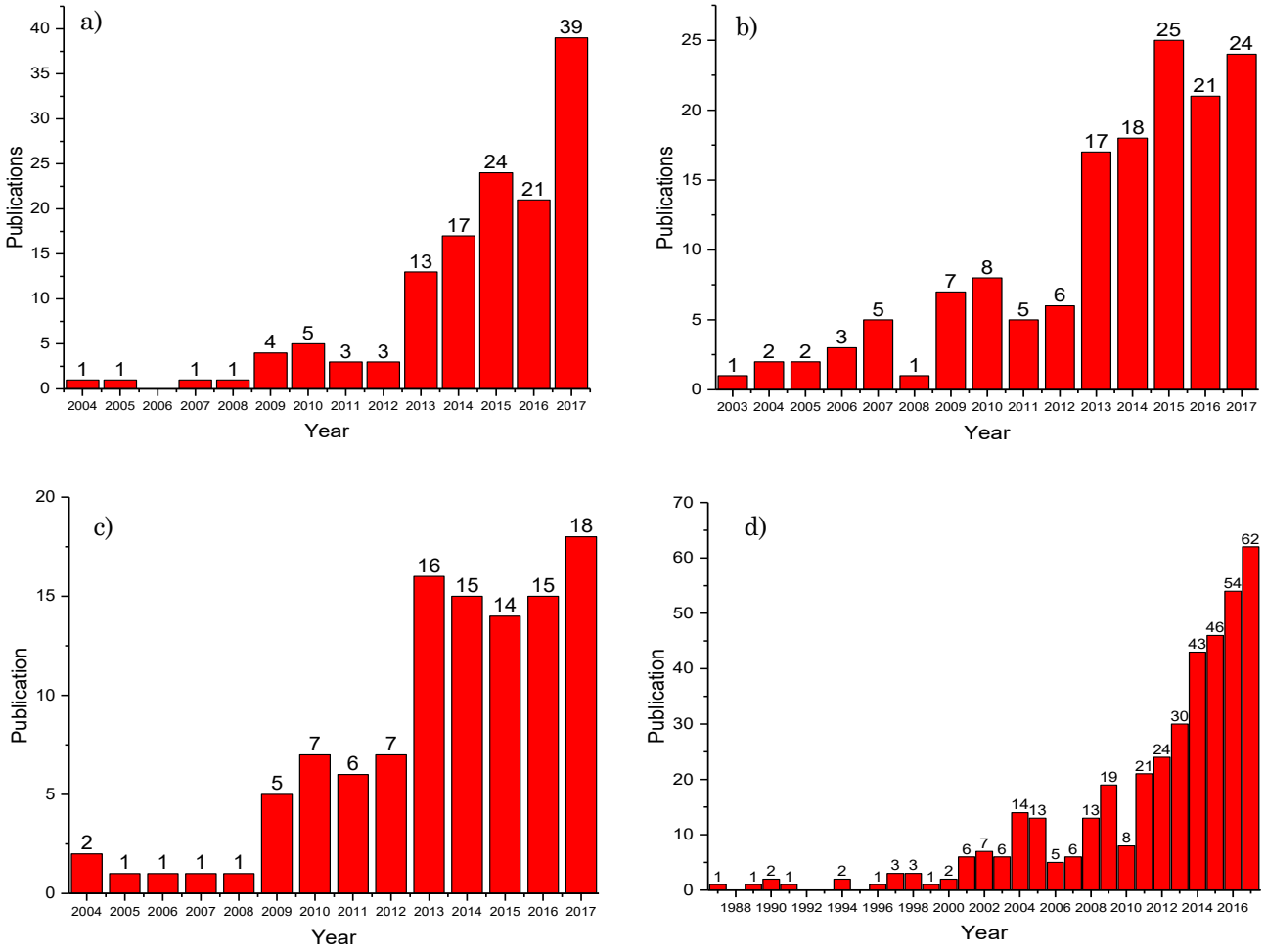

Figure 1. (a, b, c, and d) A number of research papers related to the application of the hydrothermal method, wet impregnation method, sol-gel, precipitation and co-Precipitation method in Fenton process to the wastewater treatment. Source: Scopus (December 2017)

titanate [53], Ferric giniite [54], Fe_3O_4-GO and phenol [27], $BiFeO_3$–g-C_3N_4 and lignin [55], MoS_2/Fe_3O_4 [56], Ag loaded $CoFe_2O_4/Fe_2O_3$ and R6G [57]. Figure 1 (a, b, c, and d) shows the number of research papers related to the application of the hydrothermal method [57-59], wet impregnation method [22,28,29], sol-gel method [4,17,60], precipitation and co-precipitation method [61-63] with the Fenton process in the field of wastewater treatment. Figure 2 depicts the pie chart of published papers of four different catalyst preparation methods used in the Fenton process. Figure 2 also displays that the most commonly used methods in the Fenton process are precipitation and co-precipitation method (51.12 %) till December 2017.

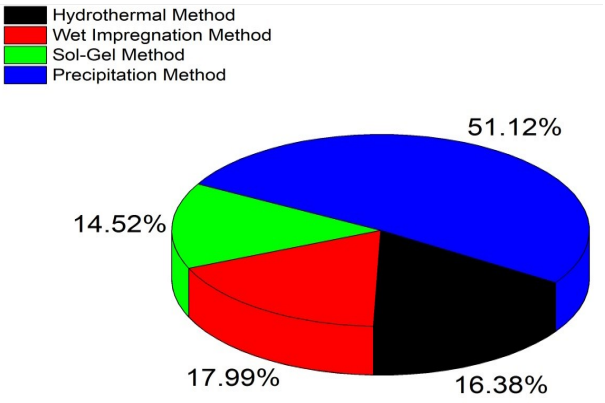

Figure 2. Three-dimensional graphical representation of published papers on different catalyst preparation methods in the Fenton process.

The characterization of any synthesized catalyst is necessary to reveal the scientific reason behind their efficiency. For instance, BET surface area investigates the specific surface area and available pore volume in the catalyst. Fourier transform infrared spectroscopy (FTIR) is used to obtain the idea about available functional group present in a catalyst with a wide range of intensity through absorbance or transmittance. Materials like metals, salts, semiconductors, minerals, and many organic-inorganic chemicals can form a crystal. X-ray diffraction (XRD) is helpful to know about the development of catalyst scientifically by measuring the

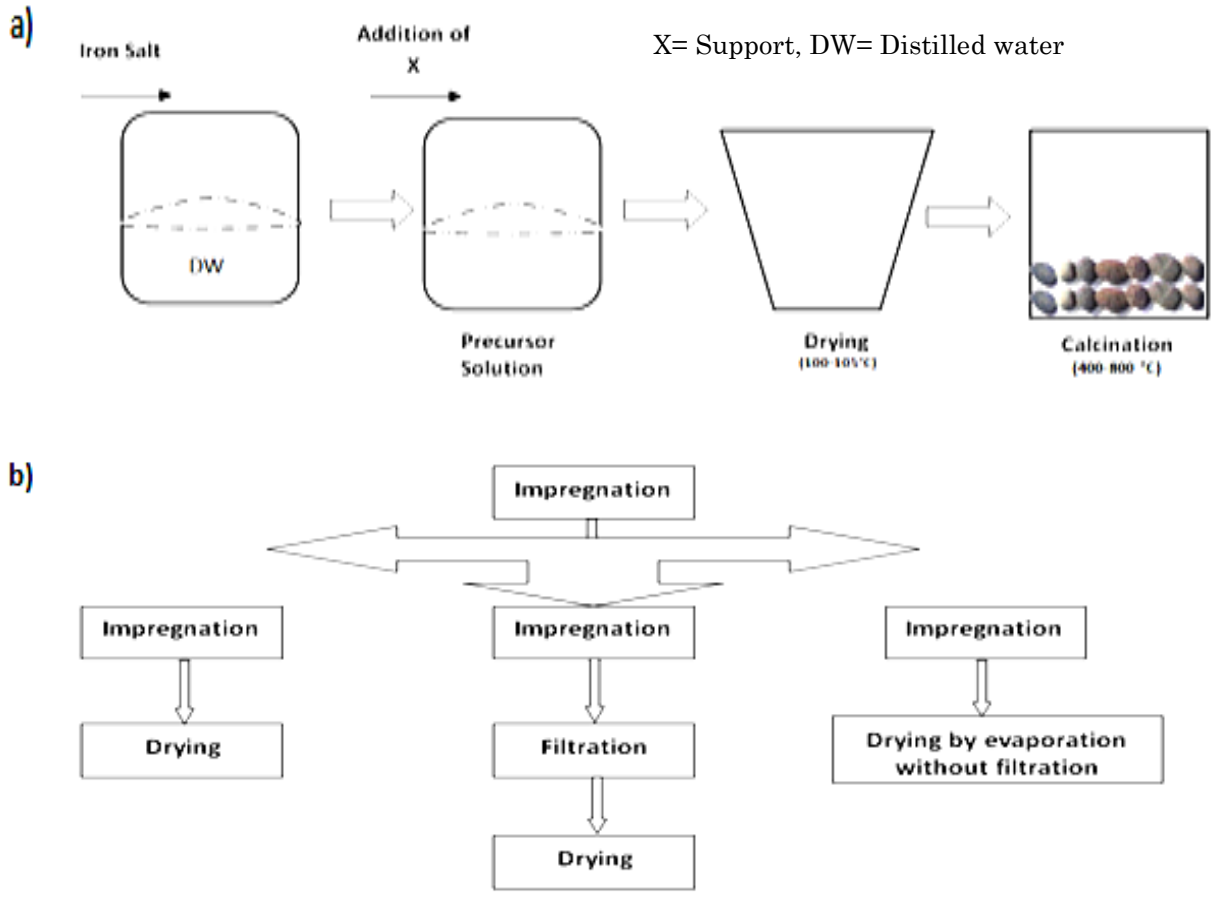

Figure 3. (a) Schematic diagram of wet impregnation process. (b) Possibilities of wet impregnation process.

intensities and angle through the diffracted beam from the material. Scanning Electron Microscopy (SEM) produces images of the sample through an incident beam of electrons on the surface of the material. The SEM can significantly achieve the resolution better than 1 nm. Thermo Gravimetric Analysis (TGA) is a technique to get information about the chemical and physical phenomena like thermal decomposition, chemisorption, solid-gas reaction and desorption, adsorption and phase transition, respectively. Temperature Programmed Reduction (TPR) profile characterization is especially useful for a heterogeneous catalyst to find the most significant oxidation/reduction condition. Raman spectroscopy observes the rotational, vibration and low frequency mode of any structural fingerprint of molecules identified by the same.

The modification of any catalyst is needed to enhance their respective characteristic and properties in the area of wastewater treatment. This can be possible with the physical and chemical modification like changing of morphology or using some modifiers. Many researchers investigated the influence of calcination temperature, acid and alkali treatment on heterogeneous catalyst.

The objective of the present review is to explore the recent development of heterogeneous catalysts on the Fenton process. Major catalyst preparation methods like wet impregnation, hydrothermal, sol-gel method, and their applications are studied in this review paper. The effect of pH and calcinations are also important in wastewater treatment. Present literature review reports the article published in last two decades on the heterogeneous catalyst for the treatment of recalcitrant, harmful organic compound and real wastewater along with reaction conditions and catalytic performances. Figure 1 and Figure 2 demonstrate the number of papers published in last 2 decades.

Present review is aimed at finding out the most significant and widely used catalyst preparation methods for the treatment of synthetic and industrial wastewater in Fenton's process. Authors also demonstrated the simplification and possible process of heterogeneous catalyst preparation methods. In addition, various parametric conditions are also tabulated to compare with each other. There are many important parameters to know about the catalyst preparation methods with respect to ageing, calcination temperature, solubility and washing (pH) as these parameters decide about the size, structure, optical, magnetic property, dimensions, homogeneous-heterogeneous nucleation and their efficiency. Present review has been focused for the same. Stability and recyclability which are important property for any useful, effective and significant catalyst has also been discussed in this work. Modification of catalyst during preparation can change their property and characteristics which have been described along with modification techniques. Factors such as pH, calcination, modifier or RPM affecting the synthesis of catalyst with respect to the surface area, pore volume, diameter of particles have been elaborated in the present review. The characterizations of synthesized catalyst are necessary to know the scientific reasons behind the outcomes which may be the next step for new research. Variety of research on synthesized catalyst have been used in Fenton's process have been discussed

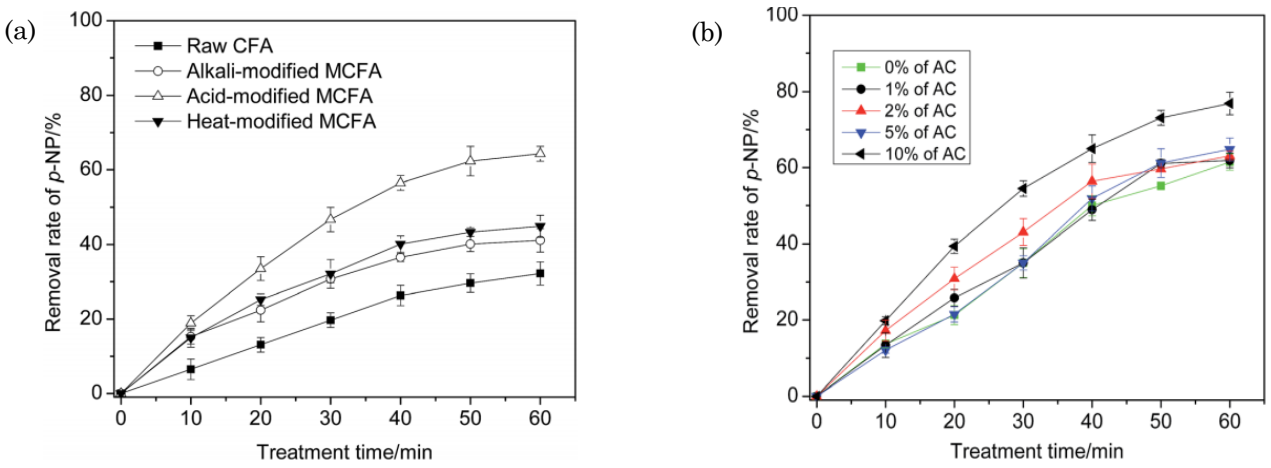

Figure 4. (a) Effect of acid, alkali and heat treatment on modification/activation of the catalyst (b) Influence of modifier on the enhancement of catalytic efficiency [68] (CFA: Coal fly ash, MCFA: Modified coal fly ash) (Reprinted with permission from Ref. [68] copyright from Royal Society of Chemistry)

Table 1. Catalyst prepared by WI method, optimum conditions and their performances

Pollutants treated	Catalyst used in WI method	Optimum Conditions				Maximum % Degradation			Ref.
		Initial Conc. (ppm)	pH	Catalyst dose (ppm)	H_2O_2 (mM)	COD (%)	Color (%)	TOC (%)	
Rhodamine B dye	Fe-SBA-15	10	3	15	-	97.7	35.1	97	[28]
Red 120	Fe-ZSM-5	10	3	0.1	-	-	98	-	[29]
Phenol	Fe/Faujasite Y zeolite	0.8-88 mg/L	5.5	1 g/L	0.007		100		[65]
P-nitrophenol	ACFA	25	3	5.5 mM/L	5	85.6	-	-	[69]
Methylene Blue	Kiesel-guhr/Fe_2O_3/TiO_2	2.9×10^{-5}	3	2	13.7	-	-	65.5	[70]
Bisphenol A	Fe-GS	100	3	20	530 mg/L	40		65	[71]
N, N-diethyl-p-phenyl diamine	Cu/Fe-SBA-15	100	3.1	10	8	83		80	[41]
Phenol	Fe-Cu allophane	5×10^{-5}M	3	-	3.5	80	-	-	[72]
Crystal violet	Fe/Clay	0.02 g/L	7	0.75	2	99	99	-	[73]
Orange II	$FeCl_3$ and $K_4[Fe(CN)_6]$	0.2 mM/L	3	6.5 g/L	9		100	60	[74]
Astrazon Blue	Fe/ACs	828 mg O_2/L	3	1.76 g/L	3.52	35.5	62.7	39.9	[75]
Coking wastewater	Cu/Fe/ TiO_2/Al_2O_3	-	-	1 g/L	14.68	65	-	68	[76]
Congo Red dye	Cu/zeolite Y	0.143 mM	7	1 g/L	52.24 mM	93.58	95.34	79.52	[77]
Acid Red B	Fe_2O_3/ACF	100	3	175	334 mg/L	-	100	43	[42]
Clofibric acid	Pd/FeOOH	25	3.3	2 g/L	0.5	-	-	82	[78]
Phenol	Fe_2O_3/Al_2O_3	5 g/L	2	1.8 g/L	0.54	-	-	80	[79]
Phenol	Fe_2O_3/γ-Al_2O_3	1 g/L	4.5	2.5 g/L	0.15 mol/L	92	-	-	[80]
P-nitrophenol	CuO/Al_2O_3	50	6	4	25	-	-	68	[81]
Acid scarlet 3R	CuO/SiO_2	0.4 g/L	3.5	6 g/L	34	90	97	-	[82]

Table 1. … (continued)

Pollutants treated	Catalyst used in WI method	Optimum Conditions				Maximum % Degradation			Ref.
		Initial Conc. (ppm)	pH	Catalyst dose (ppm)	H_2O_2 (mM)	COD (%)	Color (%)	TOC (%)	
4-chlorophenol	Fe/OMC	100	3	40	6.6	96.1		47.4	[24]
Black 5 dye	Fe/RHA	100	3	0.5 g/L	4	59.71	89.18		[83]
Reactive Black 5	Fe-AN	50	2.5	1	16	-	99	-	[84]
6-Nitryl wastewater	Fe-Cu-Y	12610 mg/L	7	7.5	3 mL	97	-	-	[85]
Diisopropanola-mine (DIPA)	Fe/TiO_2	100	1.77	-	-	80	-	-	[86]
Acid Green 25	Fe-IC	50 mg/L	3	1.25	6.7	-	95	-	[87]
Reactive black 5	Fe-areca nut	50 mg/L	2.5	1	16	-	99	-	[84]
Methyl orange	NdFeB-AC-FC	20 mg/L	3	10 g/L	0.6	97.8	-	-	[88]
Rhodamine B and 4-nitrophenol	GO–Fe_2O_3	100	2	0.2 g/L	10	-	99	76	[43]
Phenol	Fe/clinoptilolite	100 mg/L	3.5	5	5.876 mm	70	-	-	[89]
Phenol	Fe/NH4Y	100 mg/L	-	1	1.65 g/L	-	96	-	[90]
4-Chlorophenol	Fe_3O_4/CeO_2	0.78 mM	3	2 g/L	30 mm		95 4-CP	66	[91]
fparaquat	Modified activat-ed carbon	25 mg/L	3	1	12.5	92	-	-	[92]
2,4-dichlorophenol	Fe/SBA-15	100 mg/L	3	0.05 g	1 g/L	-	-	60	[93]
Polyacrylamide	Fe(III)–SiO_2	100 mg/L	6.8	1.0 g/L	200 mg/L		94 PAM	60	[46]
Phenol	Clinoptilolite zeolite	100 mg/L	3.25	15 g/L	20 mg/L	91.6	98 phenol	-	[23]
Orange G	Fe_3O_4/CeO_2	50 mg/L	2.5	2	26 mM	-	98.2 OG	-	[94]
Sulfamethazine	Fe_3O_4-Mn_3O_4/Gr	20 mg/L	3	0.5 g/L	6	-	98 smt	-	[95]
2-chlorophenol	Mesostructured silicananoparticle	50 mg/L	5.11	0.40 g/L	0.14 mM	99.9	-	-	[96]

in this review to know about the efficiency of the different processes with different parametric conditions.

2. Catalyst: Types of Synthesis

2.1 Wet Impregnation Method

Wet impregnation (WI), also called dry impregnation or capillary impregnation is a frequently used method for the synthesis of heterogeneous catalysts. In this technique, the metal precursor is dissolved in an aqueous solution. Then the same pore volume of metal-containing solution is added into a catalyst support. Due to capillary action, solution goes into the pores. After this, drying and calcinations are done to remove the volatile component. It is a process of enhancement of dispersion of active phase on support [36]. Figure 3 (a and b) demonstrates the flow diagram of WI method and possible processes.

Garcia *et al*. studied the catalyst preparation from Rose stems impregnated with iron oxide by wet impregnation method and found the excellent surface area. Significant color (98.33%) was removed only in 20 min with 3% wt of Fe [64]. Alam *et al*. reported that the synthesis of Fe^{3+}/Cu^{2+} over ZnO can be utilized for the degradation of Rhodamine B (RhB), 4-nitrophenol (4-NP) and Paracetamol. The prepared catalyst is very sensitive to visible light but the iron grafted ZnO exhibited higher activity than copper grafted zinc oxide [37]. Faujasite Y zeolite impregnated with Fe^{3+} showed excellent potential to degrade micropollutants like carbamazepine, bisphenol A, clarithromycin, carbamazepine-10,11-epoxide, triclosan, diclofenac, PFOS, estrone, naproxen, ibuprofen, lidocaine, ketoprofen. The absence of a diffraction line (in XRD pattern) of iron oxide and zero modification found on the morphology of faujasite (in SEM images) were reported. This is due to the very low temperature used for the synthesis of catalyst [65]. Figure 4 (a) displays that Acid treatment is a comparatively better option for the enhancement of catalytic activity or activation of catalyst (coal fly ash). Wang *et al*. recommended that the 12 h of impregnation is necessary for the good catalyst [66]. Material like activated carbon can be used as a modifier. With the use of the modifier, it will increase the catalytic efficiency by increasing the pore volume. Figure 4 (b) shows the % removal of p-NP using a modified catalyst. In the wet impregnation method for the preparation of appropriate catalyst, the effect of calcination and time have a significant role. For the making of a suitable catalyst, the calcinations temperature should be higher than 673 K and optimal time was measured as 12 hrs [65]. Some authors used special equipment for the preparation of catalyst like rotary evaporator device. Impregnation of iron nitrate and nanocatalyst was employed in this device with certain temperature, pressure and time [67]. Table 1 shows brief literature survey of previous research work in which catalyst was prepared by WI method.

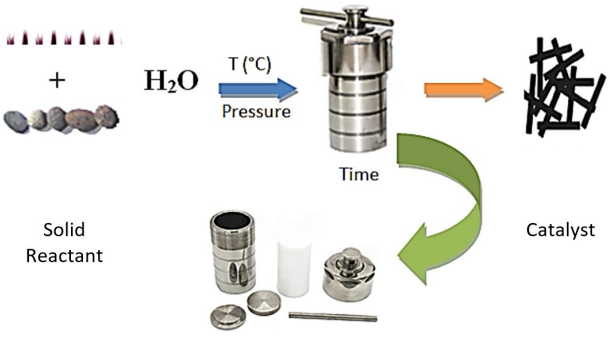

Figure 5. Schematic diagram of catalyst preparation method by hydrothermal synthesis.

2.2 Hydrothermal Method

Hydrothermal synthesis occurs with the interaction between two solids under certain temperature and pressure. For the preparation of catalyst with the hydrothermal method, Teflon lined autoclave reactor made of stainless steel is required. This method is generally used for the making of zeolites and mixed oxides when molecular sieves come contact to each other. Hydrothermal method has opened a marvelous hope for the synthesis of various dimensional catalysts with an array of monodispersed pore size and redox properties [97]. Figure 5 depicts the procedure of the hydrothermal method for the synthesis of the catalyst. Bian *et al*. studied this method and prepared catalyst was used as a Surface-enhanced Raman scattering (SERS) substrate for the detection and decolorization of RG6 through photo-Fenton catalytic method. SERS is a susceptible, nondestructive and investigative instrument which can sense analytes even a solitary particle [98]. In this study, nanorod arrays ($CoFe_2O_4/Fe_2O_3$) loaded with Ag was successfully fabricated on the carbon fiber cloth and that composite shows the bifunctional property (SERS) as well as a photo-Fenton catalyst [98]. Natural mineral (saprolite laterite ore) doped with multi-metal do not have the excellent photocatalytic activity, but it has good stability and recyclability performance. Most important

Table 2. Catalyst prepared by HM method, optimum conditions and their respective performances.

Pollutants Treated	Catalyst used in hydro-thermal method	Optimum Conditions				Maximum % Degradation			Ref.
		Initial Conc. (mg/L)	pH	Catalyst dose (mg/L)	H_2O_2 (mM/L)	COD (%)	Color (%)	TOC (%)	
p-Hydroxybenzoic acid	Fe/Pd-HNT	10^{-3} mol/L	3.1	0.1 g	0.12	52	-	-	[112]
Rhodamine B (RhB)	V-MCM-41	0.02 mmol/L	3	4 g/L	4	-	55	-	[113]
Rhodamine 6G	CuFeZSM-5	0.1 g/dm	3.4	0.15 g	40		100	51.8	[50]
Orange II	ZSM-5	0.05 g/dm^3	3.5	0.15 g	40	81.2	99.7	-	[114]
methylene blue	$Fe_5(PO_4)_4(OH)_3.2H_2O$	100 mL	4	0.5 g/L	9.8	-		-	[115]
Phenol	$Fe_8O_8(OH)_{4.5}(SO_4)_{1.75}$	100	5	1 g/L	500 mg/L	-	-	98	[26]
Methyl Orange	TiO_2/ß-FeOOH	100	4.5	0.2 g/L	0.3 g/L	-	41.2	90.09	[116]
RR195	Fe–Cr-MIL-101	100 ppm	5.5	300	136 mg/L	-	98	-	[117]
dye pollution	HPB Ba_2Na_2[HPWV 4WVI $8O_{40}$] $\cdot 26H_2O$ (BaNaPW)	0.02 mM	2.5	14.6	6	-	95	-	[99]
Methylene blue	Fe_2O_3@diatomite	20	3	0.05 g/L	90	-	99	-	[59]
methyl orange sulfamethoxa-zole	BFOs	3	3		16	-	99	99	[118]
phenol	(Fhy/MC)	100	5	0.5 g/L	30	94.2	-	-	[119]
organic pollu-tants	CoS_2/MWCNT CoS_2 black	0.112 mM	3	1	30	60	-	43	[120]
Methyl Orange	Fe–Mn/MCM-41	100	3.0±0.1	1 g/L	5	-	100	60	[121]
Dyeing wastewater treatment	MBC	100	3	0.1 g/100 mL	1 ml/L	47± 3.3	-	49 ± 2.7	[122]
acid red G	[a-Fe_2O_3]	50	2	1 g/L	30	62	98	-	[101]
benzophenone-3	CueMneO	2	7	100	1	81.5	-	-	[123]
Bisphenol A	Cu-doped $AlPO_4$	25	7	1 g/L	10	92	-	-	[124]
DDT	Ni@Fe_3O_4	1 ppm	7	0.2 g/L	50	90	-	-	[125]
methylene blue	MnO_2@SiO_2 NFM	10	6	10	15 mL	-	95	-	[126]

Table 2. … (continued)

Pollutants Treated	Catalyst used in hydrothermal method	Optimum Conditions				Maximum % Degradation			Ref.
		Initial Conc. (mg/L)	pH	Catalyst dose (mg/L)	H_2O_2 (mM/L)	COD (%)	Color (%)	TOC (%)	
methyl orange	MIL-100(Fe)/GO	50	3	0.5 g/L	8	-	98	38	[127]
Reactive Black 5	rGO/MnO_2	10 µm	5	20	6 mL	-	95	-	[128]
Rhodamine B	Amorphous Fe-Zn-oxide/hydrochar	10	6.5	0.5 g/L	10	-	96.2	-	[105]
Bisphenol A	Cu/TUD-1	100 ppm	3.5	0.1 g	90	90.4	-	-	[45]
Methyl Blue	MnO_2 nanorods	0.16 mM	6.7	1 g/L	1.45	-	100	-	[129]
Methyl Orange	CuAl-LDH	20	7	20	0.5 mL	-	93.05	-	[130]
Methyl Blue	Fe_3O_4/C/Cu	100	6.9	0.5 g/L	163.7	-	97.2	-	[131]
PFOA	Pb-BFO/rGO	50	5	1 g/L	44 mg/L	-	-	90	[132]
BPA	$BiFeO_3$	30	5	1 g/L	44 mg/L	-	-	94	[133]
MB	Fe_3O_4/SiO_2/C	50	7.5	20	1 mL	68.62	96	-	[134]
MO	Fe_2O_3/MoS_2	20	7.5	10	0.4 mL	56	99	-	[135]
MG & RhB	CuSe	20 mL	-	10	1 mL	-	96	-	[136]
Refactory Pollutants	DCAS Ns	23	7	1 g/L	10	-	92.5	73.5	[137]
C_6H_5OH	Cu-SBA-5	100	8	1 g/L	0.05 mol/L	100		66.9	[138]
MB	MnSNTs	50 ppm	2-3	20	10 mL	-	98.1	-	[139]
MB	CNTs/ Beta-FeOOH	80	4.5	0.4 g/L	0.3 g/L	-	88.9	-	[140]
RhB	$Bi_{25}FeO_{40}$	80	4.2-4.4	0.08 g	1 mL	-	98	-	[141]
BPA	d-TiCuAl-SiO_2 Ns	23	7	0.8 g/L	12	-	-	60-90	[142]
MB	Co_3O_4	10 ppm	7	1 mg	1 mL	-	100	-	[143]

Table 3. Catalyst prepared by SG method, optimum conditions and their achievements.

Pollutants Treated	Catalyst used in sol-gel method	Optimum Conditions				Maximum % Degradation			Ref.
		Initial Conc. (ppm)	pH	Catalyst dose (ppm)	H_2O_2 (mM)	COD (%)	Color (%)	TOC (%)	
organic	Solid	100	6.5	100	20 mL	80	-	-	[148]
phenol	Fe_2O_3-ZrO_2	100	7	0.8 g/L	112	-	-	56	[18]
bisphenol	N-BFO nanoparti-cles	30	5.5	0.25 mmol/L	10	94	-	-	[144]
Rhodamine B	Cu-embedded mes-oporous alumina	10 ppm	5.14	1 g/L	1000 ppm	98.53	-	-	[21]
Paracetamol	five Fe-carbon xerogels	50	6.2-6.4	100	13.8	90	-	50	[10]
Tetracycline	Fe_3O_4@void@TiO_2	40	3	0.25 g/L	0.377 M	-	75	-	[12]
Sulfide and phe-nolic compounds	CuO/CeO_2	250	3.5	1 g/L	1238 mg/L	76	-	-	[19]
Antibiotics	Fe_2O_3, TiO_2 and Fe_2O_3–TiO_2	10	2.8	2	2.5	79	-	55	[13]
Phenol	Fe_2O_3/SiO_2	1 g/L	2.7	5 g	2.55 g/L	100	-	60	[149]
Rhodamine B dye	iron molybdate	10	-	1 g/L	40	-	97	-	[30]
2-Chlorophenol	metal-doped BFO MNPsv	50	5.5	0.04 g	10	100	-	73	[150]
acid orange II	Fe-doped TiO_2	20	4	0.5 g/L	0.04 mol/L	-	99	--	[7]
Electrochemical nitrate	novel Co_3O_4/Ti cathode	100	7	50 mg/L	0.05 mol/L	Nitro-gen-85	-	-	[151]
methyl blue	Fe-GMCA	10 mg/mL	3	0.02 g	-	-	99	-	[20]
sulfamethoxa-zole	Magnetic carbon xerogels	50 µg/L	3	80	500 mg/L	-	-	42	[152]
toluene	Ba-doping in $BiFeO_3$	100	5.5	40	0.6-65	85	-	94	[153]
methyl orange	TiO_2/Fe_3O_4	100	6.5	100	0.4	-	88	-	[148]
Glycerol	$CuFe_2O_4$	68.4 mM	0.1 g/L	5 g/L	819.5	Degra-dation-40	-	-	[154]
2-chlorophenol	mesostructured silica nanoparticles	50	5	0.4 g/L	0.156	99.9	-	-	[96]
Orange I	Fe–B	0.2 mM	3	0.5 g/L	10	-	-	75	[155]

part of this study is that the leaching solution can be taken as a precursor solution for the synthesis of catalyst [58]. Similarly, HPB-3D inorganic heteropoly blue [99], MnO_2-templated iron oxide-coated diatomite [59], magnetic g-C_3N_4/a-Fe_2O_3/Fe_3O_4 composite [100], burger-like a-Fe_2O_3 catalyst [101], 3D hierarchical nanostructured hematite (Fe_2O_3) [102], MoS_2/Fe_3O_4 nano composite [56], Mixed a-Fe_2O_3/Bi_2WO_6 oxides [103], Fe_2O_3/expanded perlite (Fe_2O_3-Ep) composite catalyst [104], Fe-Zn-oxide/hydrochar [105], Ag_3PO_4/CuO composites [106], zinc oxide decorated iron oxide/reduced graphene oxide nanocomposite [107], Cu-doped $LaFeO_3$ [108], Fe(III)-tartrate/TiO_2 nano tubular [109], Fe_3O_4-GO nano composite [27], $ZnFe_2O_4$ nanostructures [110], $BiFeO_3$–g-C_3N_4 compound [55] were prepared by the hydrothermal method and used as photocatalysts. Recently, some researchers investigated that the metal doped Fe_2O_3 catalyst has good stability and potential to enhance the photo degradation [111]. Table 2 shows the brief literature survey of previous research work in which catalyst was prepared by hydrothermal method (HM) method.

2.3 Sol-gel Method

Sol-gel is the second largest method used for the preparation of xerogels or aerogels. Sol is a colloidal suspension of solid particles in a solution with the particle range from nm to µm size. Gel is defined as the solid surrounded by liquid. In the first step for the synthesis of catalyst monomer, metallic oxide reacts with water and produce a polymeric gel which is considered as an oxide gel. Then in the second step, condensation occur which forms gel by dehydration and create a Metal-O-Metal bond. The third step is a formation of a gel by drying or aging which produces a cross-linked gel. During the progress of gel formation, viscosity also increases till the sol-gel transition point. Then with further increase in viscosity in cross-linking results in maximum density which occurs by aging and drying. The role of pH is very important in the synthesis process because lower value of the same parameter gives a lower cross-linking substance. Similarly, aging, temperature, water alkoxide ratio, alkyl group (length, molecular weight) and oxidation state are also important parameters. One of the parameters is gel structure which completely depends on hydroxyl group present in the gel after drying. Figure 6 displays the fundamental phenomena of the sol-gel process.

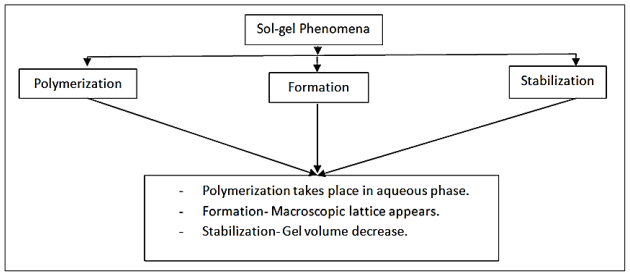

Figure 6. The basic phenomena of the sol-gel process.

Alhmoud *et al.* investigated that mixed oxide containing iron has great efficacy to degrade phenol and their derivatives [2,18,19,144,145]. The author used different metals and synthesized catalyst by sol-gel method for example: $CuFe_{1.2}O_{2.8}$, $BaFe_{7.2}O_{11.8}$, $BaFe_{7.2}Cu_2O_{13.8}$, $BaFe_{5.4}V_3O_{16.6}$, $BaFe_{4.8}Cu_2V_3O_{17.7}$, and $Ag_2Fe_{5.4}V_3O_{16.6}$. In addition, it was also found that catalytic activity was suppressed with the increase of temperature [17]. Another researcher developed a catalyst rGO-Fe_3O_4-TiO_2 with a ratio of 1:1:2 and about 99% of dye was degraded in only 6 minutes [4]. Similarly, many scientists worked with the prepared catalyst by sol-gel method for degradation of dye like Rhodamine B and Cu-Embedded Alumina [21], acid orange-II and Fe-doped TiO_2 [7], methylene blue dye and Ag-SiO_2@-Fe_2O_3 [146], Orange G and TiO_2/stainless steel mesh photo-electrode [147], methyl orange and TiO_2/Fe_3O_4 [148]. Table 3 shows the brief literature survey of previous

Table 4. Precipitation parameters and their effects on seeding [2].

Parameters	Effects on crystal
pH	Phase
Solution composition	Phase, purity, precipitation composition
Aging	Purity, crystallinity, textural properties
Additives	Textural properties
Temperature	Phase, textural properties
Mixing sequence	Precipitate composition, homogeneity
Solvent	Textural properties, crystallinity
Super saturation	Particle size, rate of precipitation
Precipitating agent	Phase, homogeneity
Anion	Morphology, textural properties

Table 5. Catalyst prepared by (PPT and CO-PPT) method, optimum condition and their achievements.

Pollutant Treated	Catalyst used in precipitation and co-precipitation method	Optimum Conditions				Maximum % Degradation			Ref.
		Initial Conc. (ppm)	pH	Catalyst dose (ppm)	H_2O_2 (mM)	COD (%)	Color (%)	TOC (%)	
NiZn	Fe/L	1 mM	7	174	10	67	-	100	[169]
Thallium	$FeSO_4 \cdot 7H_2O$	500 µm	2.5	21.58	53.96	96.54	-	70.42	[170]
Methyl Orange	Fe_3O_4/MWCNTs	50	2	2 g/L	19.38	-	-	-	[159]
Methylene Blue	MFe_2O_4	10	-	100	4 mL	-	99.5	-	[157]
Acid orange 7	K-FeOx-2/2-3H	25	3	3 g/L	5	--	80	-	[171]
Organic Pollutant	Fe_2GeS_4	20	7	0.3 g/L	50	74.2	MO=66.2 MB=56.3	-	[172]
4-Bromophenol	Se-doped CuO NPs	0.2	-	10	0.038 M	99.5	-	-	[63]
Humic acids (HAs)	ferrioxalate complexes	100	2.8	40	42	HA 95	-	-	[173]
Chlordimeform insecticide	Fe_3O_4-Cs	37.5	3	0.5	0.104±0.001	-	-	80	[62]
Methyl Orange Sulfamethoxazole	BFO/H_2O_2/PMS	3 mg/L	3	0.12 g/L	40	-	99	99	[118]
Sulfate	SBR	200 mL	2	8 mM/L	40	77.9	-	-	[174]
Benzophenone-3 (BP-3)	CueMneO	2	7	100	40	81.5	-	-	[123]
Phenol	$NiFe_2O_4$	250	3	2 g/L	120	95±3.4	-	-	[175]
RhB	Fe_3O_4/Al-B	40	3	1 g/L	50	RhB 99.9	-	-	[168]
Phenol p-Nitrophenol	Fe_3O_4/MWCNT	100	3	1	10	99.20	-	-	[167]
SDBS	ZVI	60	6	2 g/L	-	-	-	77.8	[176]
Alkalinity Ammonium nitrogen	Fe^{2+}	100	2.8	60	120	58	DOC=60 TSS=88	-	[177]
Congo red	Cobalt–copper oxalate	100	7	100	100 mg/L	-	100	-	[166]
levofloxacin	ferrioxalate complexes	20	5	2	20 mg/L	DOC=86 LEV=71	-	-	[178]
Methyl orange	$NiFe(C_2O_4)_x$	20	3-10	0.4 g/L	10	-	98	-	[165]
catechol	Fe_3O_4-CeO_2	10 mM	2.4	50	30	89.2	-	-	[164]
Reactive Black 5	modified cigarette filter (MCF)	50	3	1 g/L	100 mg/L	-	99.09	-	[179]
Enrofloxacin	Fe^{2+}	100	2-3	28.3	738 mg/L	-	-	> 58	[180]

Table 5. … (continued).

Pollutant Treated	Catalyst used in precipitation and co-precipitation method	Optimum Conditions				Maximum % Degradation			Ref.
		Initial Conc. (ppm)	pH	Catalyst dose (ppm)	H_2O_2 (mM)	COD (%)	Color (%)	TOC (%)	
Methylene blue Rhodamine B	La-Fe MMT	100	Neutral	0.1 g/L	30	75	MB=97 RhB=96	-	[163]
Dye	diatomite/Fe_2O_3/TiO_2	2.9×10^{-5}	7	2 g/L	210 µL	-	96	-	[162]
nitrobenzene	Co-Fe LDH	20 µL	2.7	1 g/L	500 mg/L	Nitrobenzene 100	-	75	[161]
Reactive Yellow 15	Fe/CuO		2	4 g/L	50	-	98	-	[160]
Micropollutants	Fe^{2+}	100	3.72	1,755	26,422 mg/L	54	-	Micropollutants=90-99%	[181]
p-arsanilic acid (p-ASA)	Fe^{2+}	10	3	0.53 mM/L	2.12	p-ASA=100 %	-	-	[182]
Phenol	Fe_3O_4-GO	20	5	0.25 g/L	10	98.8	-	81.3	[27]
Methyl Orange	Fe_3O_4@HG	10	3.5	3	1.2 mL	-	87.68	-	[183]
Methylene Blue	$BaFe_{12}O_{19}$	10	-	0.75 g/L	12	-	70.8	Mineralization=63.7%	[184]
reactive brilliant blue	Fe-Mn-sepiolite	50	2.5	0.4 g	3 mL	-	-	91.98	[185]
glycerin	Fe^{2+}-HA Fe^{2+}-BQ	100	3	5 mM/L	50	-	-	90	[186]
beverage industrial effluent	Fe(II)/PS	500	2.9	375	4000 mg/L	Mineral=76	-	93	[187]
Orange II	Fe_3O_4/Al-Fe-P-B	0.23 mM/L	4	1 g/L	1	92.2	99.3	-	[188]
2,4,5-trichlorophenoxyacetic acid	cLDHs	100	3.8	4 g/L	2.73	-	-	80-95	[189]
cibacron brilliant red 3B-A (BR3B-A)	$Fe_{78}Si_9B_{13}$	0.02 mM	2.5	14.6 mg	6	-	100	-	[99]
BPA	Fe_3O_4 -TA	0.5 µM	6.6	1 g/L	10	BPA=80 %	-	-	[190]
Sludge	MFeNp	100 mL	3	50 mg/g	500 mg/g	Sludge=85.9 %	-	-	[191]

research work in which catalyst was prepared by sol-gel (SG) method.

2.4 Precipitation and Co-precipitation Method

Two basic things of precipitation are nucleation and growth. When high supersaturation is achieved then nucleation comes into the picture (formation of solid crystal) and growth means approaching an equilibrium state with the new phase. Formed crystal could be homogeneous or heterogeneous. Homogeneous nucleation occurs when molecules interact with each other with the same phase under supersaturation condition and irreversible crystal is formed while in heterogeneous nucleation. For the successful precipitation, some necessary parameters should be controlled like initial pH, pH variation during the process, the rate of addition of solution, order, types of mixing, maturation etc. Due to its simple nature and cost-effectiveness, this method is the most used all over the world. Few disadvantages are product separation after precipitation, higher salt amount present in solution, etc. [97].

In the co-precipitation method, two different ions (cation and anion) are associated with a fixed composition. If the same ions interact, then characteristic (solubility constant and supersaturation value) and properties of formed seed will also change with time. For the preparation of mixed oxide, solubility is a very important factor in the case of co-precipitation. Similar to precipitation, in the co-precipitation also pH has a great role. There are two methods for seeding by the co-precipitation method: a) constant pH method, and b) variable pH method during the process. Stirring can also change the property of crystal in the precipitation. Parameters and their effects on crystal are listed in Table 4 [97].

Vinosha *et al.* investigated the effect of different pH (9-12) on crystal formation in terms of structure, optical and magnetic properties of $CoFe_2O_4$ nanoparticle which was prepared by co-precipitation method. Authors also investigated that the prepared catalyst will be much effective in the Fenton process using methylene blue as a model pollutant [61]. Selenium has a photo absorption property and the great efficiency to improve the in-situ generation of hydroxyl radical. Sharma & Dutta synthesized the catalyst using selenium and studied their optical, morphological and structural properties of Se-doped CuO NPs nanoparticles [63]. Gan *et al.* prepared a catalyst by oxidation, reduction and co-precipitation, and that catalyst exhibits great catalytic ability and efficient reusability performance [94]. The researchers studied the application of prepared catalyst by precipitation and co-precipitation method in the various field like color removal and recalcitrant organic compound degradation. Some examples of dye as model pollutant, and prepared catalyst are $Ni_{1-x}Zn_xFe_2O_4$ and methylene blue [156-158], methyl orange and Fe_3O_4/MWCNTs nanocomposites [159], Reactive Yellow 15 and Fe/CuO catalyst [160], nitrobenzene and Co-Fe layered double hydroxide (Co-Fe LDH) [161], methylene blue and Magnetic diatomite (Kieselguhr)/Fe_2O_3/TiO_2 composite [162], RhB and methylene blue (MB)

Table 6. The possible structure of matter and their properties.

Shape	Figure	Properties
Sphere		Low manufacturing costs The relatively high-pressure drop Large diffusion length HDS, Methanation
Granules		Not common, Low-surface-area catalysts Ammonia Synthesis, Formaldehyde
Pellets		Regular shape; Most common Good strength. CO shift Hydrogenation
Extrudates cylinder		Low-pressure drop; Poor strength HDS
Ring		High strength; Low-pressure drop Small diffusion length. Steam Reforming
Monoliths ceramics		Low pressure drop; Insensitive to dust; Small diffusion length Exhaust gas cleaning

and La-Fe montmorillonite (La-Fe MMT) [163], orange G and Fe_3O_4/CeO_2 composite [94], catechol and Fe_3O_4-CeO_2 metal oxide [164], methyl orange and Ni-$Fe(C_2O_4)_x$ [165], Rhodamine B dye and Iron molybdate $Fe_2(MoO_4)_3$ nanopowders [30], congo red and cobalt-copper oxalate and cobalt oxalate nanofibers [166], Phenol and Fe_3O_4/MWCNT [167], rhodamine B (RhB) and Al pillared bentonite-Fe_3O_4 nanocomposites (Fe_3O_4/Al-B) [168]. Table 5 shows the brief literature survey of previous research work in which catalyst was prepared by precipitation and co-precipitation (PPT and CO-PPT) method.

3. Modification and Application of Modified Catalyst in the Fenton Process

Modified Fenton's catalyst (MFC) is directly related with the Fenton's chemistry. British chemist Henry J.H. Fenton first established the use of Fenton's chemistry (1894), through the degradation of tartaric acid by the use of iron, hydrogen peroxide under acidic conditions. MFC process was developed to overcome the application of Fenton's reagent in its conventional form (such as: acidic pH, iron leaching, sludge formation, reusability, *etc.*). The main aim of modification of Fenton's catalyst is to stop iron leaching and chelating. To prevent pH fluctuation during process, modification of Fenton's catalyst can be done at normal pH of 5-7. Chelated catalyst has a better attraction towards the iron compared with other metals, hence the iron loss is negligible. The fundamental Fenton reaction is between Fe^{2+} and hydrogen peroxide and produces hydroxyl radical (•OH), Fe^{3+}, and OH^-. Modified Fenton's processes produce superoxide radical anion ($O_2^{\cdot-}$) or hydroperoxyl ion (HO_2^-) which endorses the chemical reaction. Similar to hydroxyl radical, superoxide and hydroperoxide anions are also responsible for the oxidation and adsorption [192].

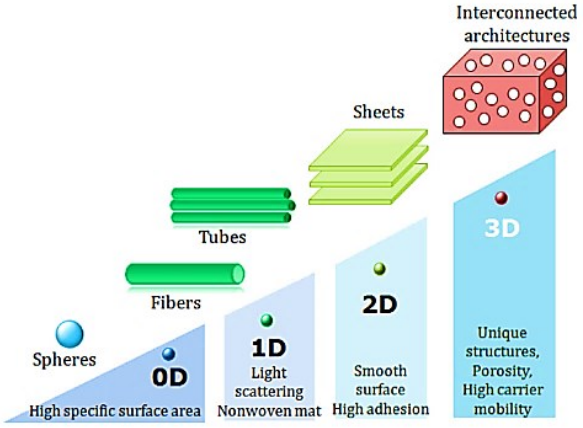

Figure 7. Various dimension and their expected properties [203] (Reprinted with permission from Ref. [203] copyright from Elsevier).

To enhance the catalytic efficiency, many researchers have been working on the modification of catalyst. Reyes *et al.* used two different ligand-based iron complex and compared their efficiency with the Fenton process. They found that modified Fenton's reagent is more efficient (at neutral pH) than simple Fenton reaction (at low pH) [193]. Textile effluent contains dye, surfactants, additives, and hazardous matter. Darshna & Yogesh used fly ash along with iron dust instead of iron salt for the degradation of color and chemical oxygen demand (COD) and got significant results [194]. Jennifer *et al.* employed a novel technique, rotating disk-slurry electrode (iron salt on the electrode and activated carbon) for the preparation of catalyst and examined their performance [195]. Mansoorian *et al.* studied both the process (Fenton and modified Fenton) for the dye decolorization with the same operating parameters and observed that modified Fenton's reagent is more efficient [196]. Similarly, Ganesan *et al.* (decolorization of textile dyeing) [197], Lewis *et al.* (degradation of trichloroethylene) [198], Wang *et al.* (degradation of p-nitrophenol) [66], Lee *et al.* (Degradation of phenol) [199], Barbusinski *et al.* (decolorization of dye wastewater) [194], Zhao *et al.* (removal of textile dyes) [200], Pradisty *et al.* (degradation of phenol) [201], Tony *et al.*, (mineralization of an oil-water emulsion) [202], Sadek *et al.* (the treatment of effluents from paint industry) investigated on modified Fenton's reagent [67].

3.1 Physical Modification

The physical modification is directly concerned with the study of morphology. The term morphology is related to the shape, structure, and form of material. The main aim of modification of the catalyst is to enhance their catalytic activity. The shape of any matter could be zero-dimensional, 1-dimensional, 2-dimensional, or multidimensional. Figure 7 shows the various dimension and their expected properties. Similarly, the matter could be of various type shapes like a sphere, pellet, ring, monolith, wagon wheel, monolith, extruded cylindrical, gauzes, *etc.* Table 6 shows the various shape and their properties.

Lee *et al*. reviewed especially on the modification of TiO_2 including metal, carbon or non-carbon material incorporated. Photocatalytic activity can be enhanced by the optimization of structure and size of the matter. The shape of TiO_2 catalyst with nanoscale can increase the adsorption capacity which is very helpful to the wastewater treatment, particular in Fenton's process. In addition, photocatalytic performance gets affected on the surface of TiO_2 dominant behavior of the e^-/h^+. Compared to the unmodified catalyst, modified catalyst showed the diversity of photocatalyst characteristics and significant catalytic activity performance. Similarly, compared to particle form, nanotube structure TiO_2 exhibits great potential to degrade recalcitrant organic compound and mineralize them into the non-toxic compounds. Nano-sized materials have the high specific area, ability to charge separation on the catalyst surface, enhanced oxidative property along with opacity, but directly this cannot be applied in wastewater treatment due to the aggregation of nano-particle [203]. Apart from the titanium, ferrite spinel has also excellent potential in the field of advanced oxidation technology. Ferrite spinel consists mostly of divalent ion which is distributed in the cubic close packing of tetrahedral or octahedral coordination sites. Catalytic performance is directly related to the oxidation and reduction property and distribution of metal ion on the configuration [204]. In similar way, metal ion ligand also has efficacy to convert H_2O_2 to hydroxyl ion due to the electron transfer mechanism in Fenton's reaction. Lee *et al.* tried to modify the surface of WO_3 with iron, platinum, Nafion, and combination of these. The authors found the best combination to degrade the 4-chlorophenol was WO_3/Fe(III)/H_2O_2 system [205].

3.2 Chemical Modification

Chemical modification (doping) is nothing but the addition of impurities, either it can be metal, non-metal, cation or anion to nanomaterial in order to enhance their potential and efficiency. The general importance of any nanomaterial lies in its good optical behavior. So, this property can be achieved by shifting of band gap from the ultraviolet region to the optical region and narrowing of band gap can be done by the doping. The main aim of doping is to increase the electrical and optical properties. Doping is the only method by which we can change the composition of nanocatalyst. Doping alters the morphological, magnetic, optical, structural and electrical properties of nano photocatalyst and also enhances the potential. Three types of doping are displayed in Figure **8**. More than 40% of the photon comes under the visible light range covering large band area. The direct application of nanomaterial is quite impossible due to the activation of nanomaterial in the UV region. In this situation, a nonmetal comes into the picture to support the absorption capacity of nanocatalyst. Nonmetal co-doping has also synergistic advantages like

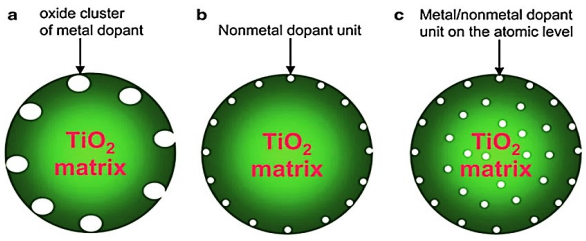

Figure 8. Different types of doping.

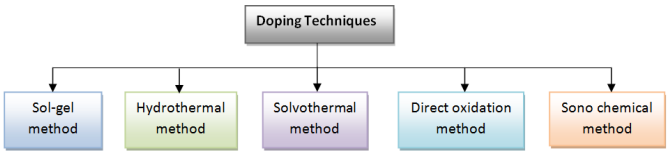

Figure 9. Various doping techniques.

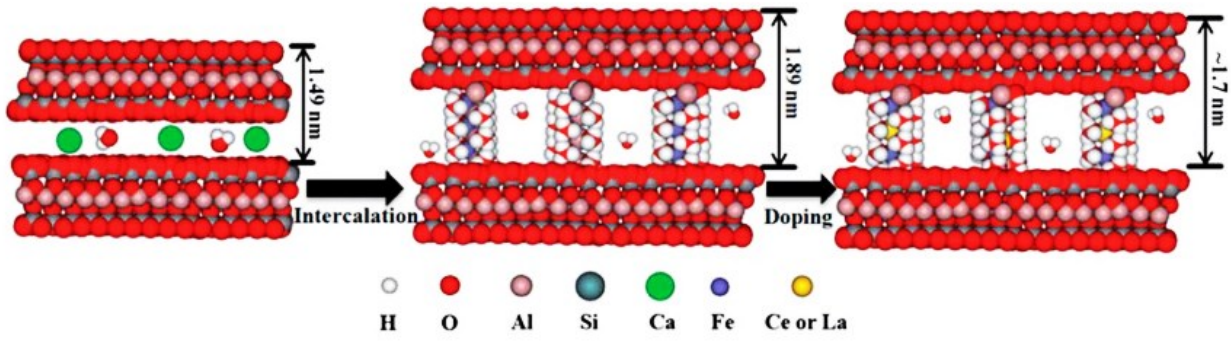

Figure 10. The insignificant doping. Ce or La was used as a doping material (Reprinted with permission from Ref. [206] copyright from RSC Advances).

high visible responses, charge separation, *etc.* [3]. Various techniques for doping are shown in Figure 9. Sol-gel and hydrothermal method have already been discussed in the previous section.

In the solvothermal method, non-aqueous solvent can be applied and this is the only difference between hydrothermal and solvothermal methods. The higher temperature is used in solvothermal method compared with the hydrothermal method and it's a one of the major advantages of this process. Direct oxidation method is mostly applicable in the field of the fuel cell. Ultrasound has a great potential to the synthesis of high surface area nanomaterial. A small amount of doping is not that much significant as shown in Figure 10 [206]. Doping techniques cover the major area to prepare nanomaterial but it is not discussed in details here.

4. Factors Affecting the Synthesis of Catalyst

In this section, the effect of parameters, like pH, calcination, and modification during catalyst synthesis and in treatment processes, will be discussed.

4.1 Effect of pH

For the synthesis of catalyst, some researchers used acid medium and some researchers used alkali. It depends on the method of preparation and in precipitation method alkali medium is used. It can be judged by taking modifier or activator. Wang *et al.* demonstrated that acid modified catalyst is more efficient than alkali [66]. They investigated that during the acid wash, alkaline catalyst gets neutralized by acid and also observed the increased surface area and pore volume, i.e. higher exposed area for catalytic reaction. But in case of alkali modification, crystal structure is damaged due to the elemental disturbance in the catalyst. The alkaline catalyst increase the pH of wastewater which could also create some problem during the treatment of wastewater. Therefore, it is concluded that acid washing is an efficient process to increase the capacity of catalyst [68]. Liang *et al.* studied the effect of the precursor pH on catalyst structure as well as on photocatalytic performance. They found that pH is responsible to change morphology, structure, and property of catalyst. Less pH has strong visible light absorption capacity. Figure 11 (a) shows the influence of catalyst prepared at dif-

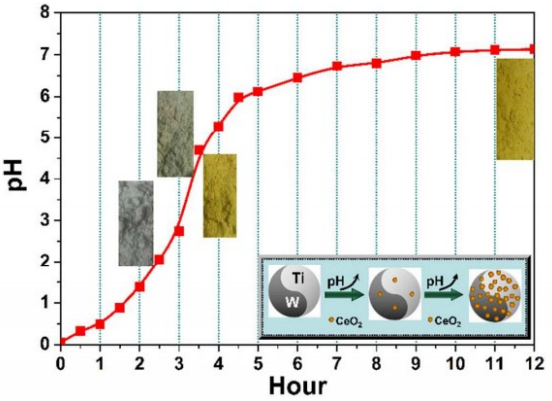

Figure 12. The synthesis of the catalyst at varying pH at different time by precipitation method [208] (Reprinted with permission from Ref. [208] copyright from RSC Advances).

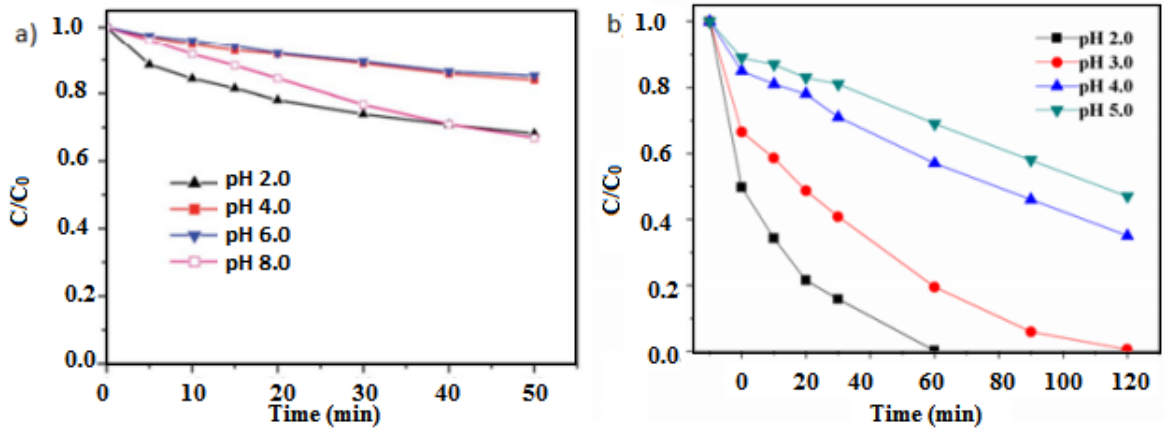

Figure 11. (a) The effect of different pH on the degradation of Orange II [207] (b) Catalytic performance of heterogeneous catalyst at different pH (Reprinted with permission from Ref. [209] copyright from RSC Advances).

ferent pH on degradation of Orange II by photocatalytic activity. Catalyst prepared at pH 2 exhibits higher degradation in lesser time as shown in Figure 11 (b) [206,207]. Huang *et al.* demonstrated that change in characteristics of the catalyst with a variation of pH at different times as shown in Figure 12. They found that with the increase of pH and time, color shifted from light yellow to yellow after 12 hours. pH can also affect the initiation, promotion, inhibition and direct reaction rate constant of any treatment processes [208,209]. Microscopic results showed that acidic medium can produce the smooth and regular structure. With the increase of pH, the size of the particle also increases, but in basic medium size gets decreased [105].

4.2. Effect of Calcinations

In this section, the effect of temperature on catalyst properties as well as on treatment processes are discussed. Morphology, structure, crystallinity and surface area are significantly affected with the increase in temperature.

In case of TiO_2 nanopowder, anatase phase powder was obtained in the temperature range of 250-500 °C, while above 600 °C rutile phase powder was formed. But with the increase in temperature, surface area gets decreased. Anatase and rutile phase showed the different result in size distribution. The size of anatase phase powder was increased with the higher calcinations temperature, but in the case of rutile phase, size got increased very slightly [210,211]. Up to 300 °C, there is no change in structure, crystallinity, and morphology. Crystallinity enhancement and impurities removal occur when calcinations temperature of material was increased to more than 300 °C. Due to this, photocatalytic activity is also increased [212].

The calcinations influence the reusability and hydrogenation capability of catalyst [213]. Zhang *et al.* investigated phenol degradation through the different calcined catalyst. In the range 400-600 °C, catalytic performance was decreased due to the damage of internal voids. As a result, the availability of active sites becomes very less and decreases the active material in the solution. Therefore, it minimizes the degradation efficiency of the catalyst. Optimized calcinations of catalyst improves the adsorption capacity as well as increase the surface area by removing the unstable stratification [214]. Calcination is also responsible to maintain the rigidity. Wang *et al.* used three different temperatures to study the rigidity of metal coal fly ash. The optimized temperature was 723 K (Figure 13 (a)), as at this temperature pores have not been broken and along with that surface area was also increased with rigidity [66]. With the increase in calcinations temperature, evaporation occurs, gas produced and spread rapidly over the surface. As a result, removal of pollutant gets decreased which shows that the surface area and pore size get

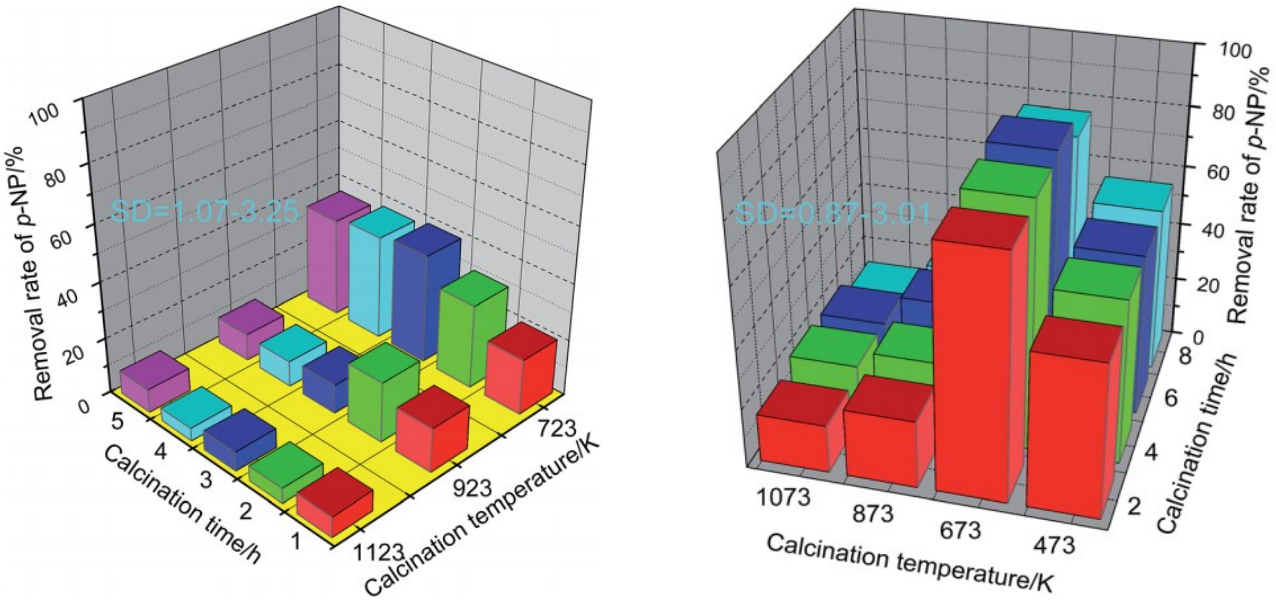

Figure 13. (a and b) The 3-dimensional view of the adsorptive and catalytic performance on the pollutant removal, with respect to calcinations time and temperature [68] (Reprinted with permission from Ref. [68] copyright from RSC Advances).

affected. Therefore, adsorption capacity is decreased [68]. Figure 13 (b) displays catalytic performance at different calcination temperature. At low calcined catalyst, the stability of iron ion on the support material becomes weak and higher calcinations create a problem like loss of strengthening and uneven distribution of catalyst particles, etc.

On similar way, Wang *et al.* also worked on the phenol degradation and hydrogen peroxide decomposition with varying temperature. Calcinations at 550 °C was observed as optimized value for the degradation as well as decomposition of H_2O_2. Iron gets dissolved with the increase in temperature from 400 to 750 °C, 0.698 to 0.149, respectively. Effect of calcination can also be seen from XRD pattern which corresponds to structural alteration during phase change [58].

4.3 Effect of Modifier

Modifier plays a significant role on the preparation of the catalyst. The modifier can change the size, structure, stability, activity and surface area of the catalyst. There are various methods by which modifier can be applied in precipitation method, impregnation method, chemical vapor deposition method, hydrothermal method etc. It could be alkali metal, transition metal, zeolites or oxide form the element. Alipour *et al.* investigated that the addition of modifier decreases the surface area, but improves the activity and stability of the catalyst [215]. With the modifier, effective photodegradation efficiency was obtained compared to without modifier [216].

5. Characterization of Synthesized Catalyst

5.1 SEM Analysis

Scanning Electron Microscopy (SEM) images tell about the surface morphology of material which gives an idea about the structure (porous-non-porous, glossy, honeycomb) and shape (spherical) [68,217]. The surface morphology shows that all the constituents of the catalyst are distributed throughout without any major migration or phase segregation. The SEM images confirmed that pores are not significant in the synthesized catalyst [289]. This is one kind of microscopic analysis, which provides direct visual and reliable images. Figure 14 (a,b,c,d) is a demonstration of SEM images of iron-carbon xerogels with multi-dimensional and different sizes. Small incorporation of any other material and their effects can be visualized in the same figure (Figure 14 (b)). In addition, it also shows the rare or denser structure, smaller and larger particle size can also be seen when some new materials are added (Figure 14. c). Figure 14 (d) shows the image after polymerization which is highly dense and cross-linked structure [10].

Elemental analysis (atomic % and weight %) can be obtained when SEM connected with Energy Dispersive X-ray spectroscopy (EDX). EDX is also known as EDS, can be used to show or map one compound to another as shown in Figure 15 [7]. Generally, the magnification of any material through SEM can be in the range of 10^5-10^6. For visualization of higher magnification, field emission-scanning electron microscopy (FESEM) is done. FESEM gives the knowledge of roughness or smoothness of material or particle [68]. Ramli *et al.* [86] reported that the method of preparation of catalyst can also change the morphology as shown in Figure 15 (d and e).

5.2 XRD Analysis

XRD is one of the most important instruments to reveal the crystallographic information. XRD analysis indicates the primary phase in the catalyst and the diffraction lines remain unchanged by the addition of impreg-

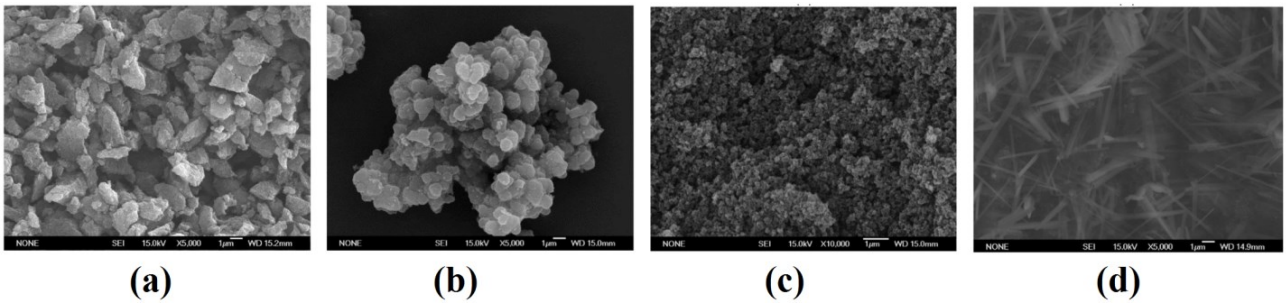

Figure 14. (a,b,c,d): The formation of iron-carbon xerogel [38]. The sizes of microbeads are 3μ and 650-830 μ with respect to (a) and (b) (Reprinted with permission from Ref. [10] copyright from Elsevier).

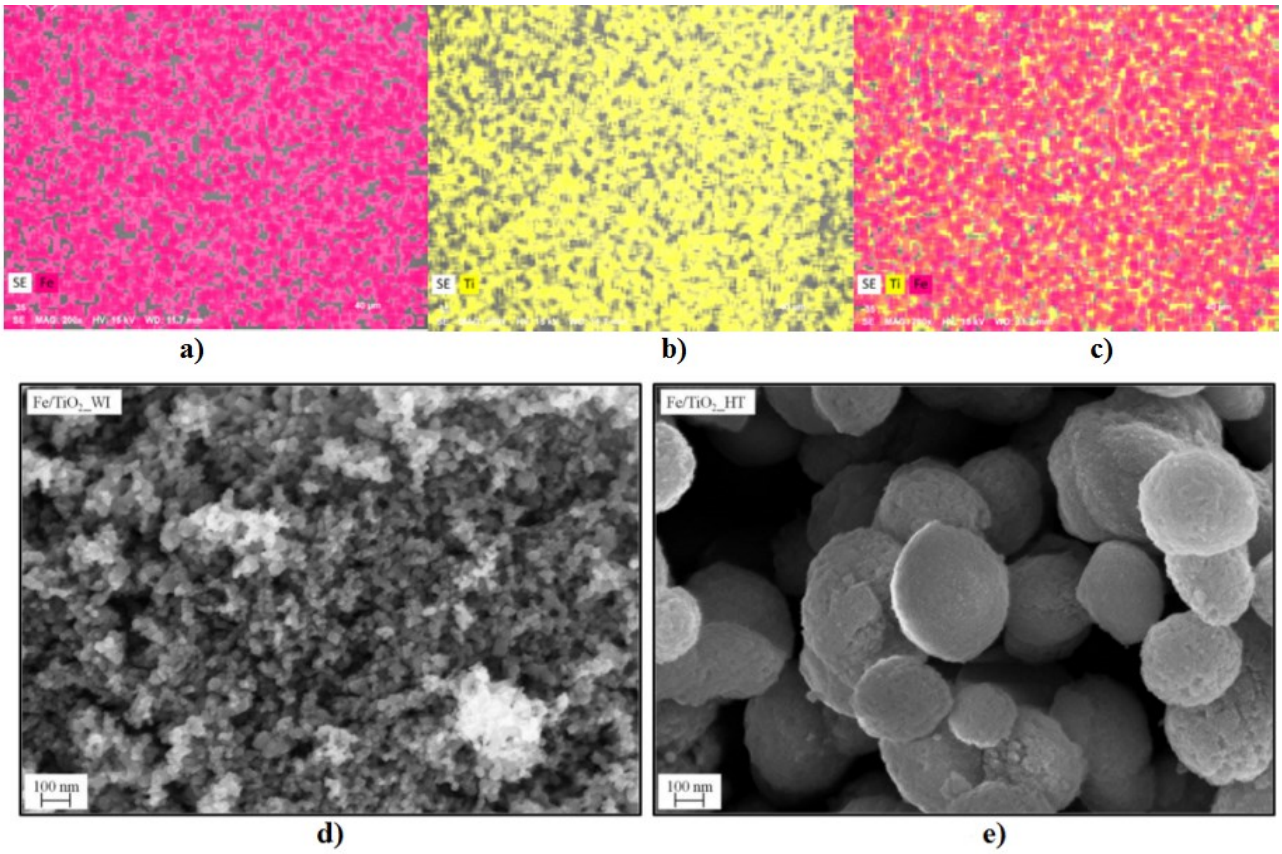

Figure 15. The red color showing iron (a) and yellow color showing is Titanium (b). Red color distributed over Titanium (c) [7]. Figure d and e illustrate the morphology of catalyst (Fe/TiO_2) synthesized by wet impregnation and hydrothermal method respectively with 50×10^3 magnification (Reprinted with permission from Ref. [7] copyright from Elsevier).

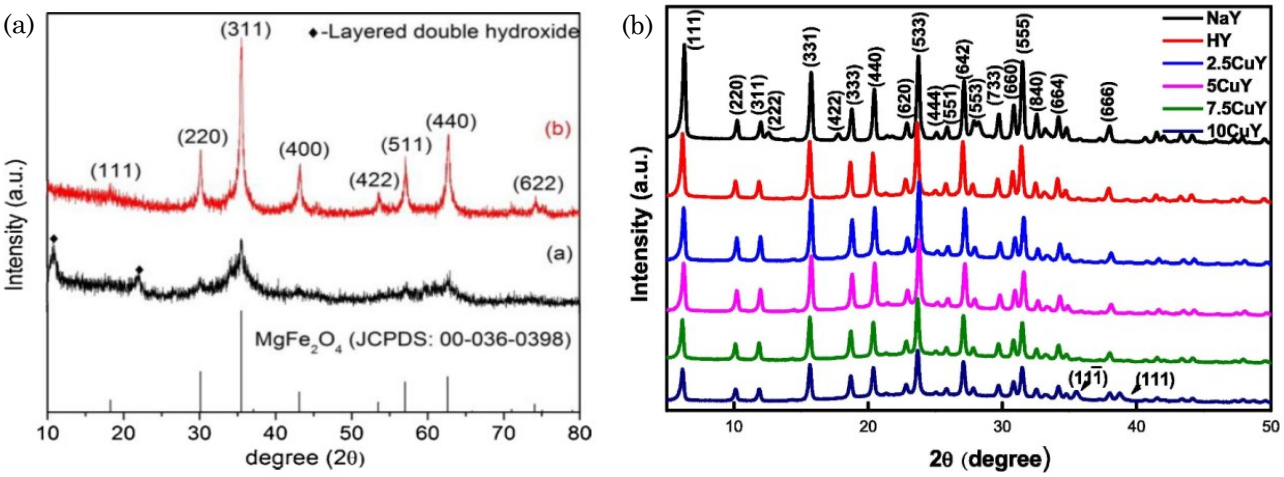

Figure 16. (a) The XRD pattern of the prepared catalyst by hydrothermal method. The black and red pattern shows the before and after calcination (550 °C for 2 h). Before calcination (black pattern) only four peaks were found at the angle of 30.1 (220), 35.5(311), 57.0(511), 62.6(440) and two more peaks. After calcination, a red pattern shows highly enhanced peaks [58]. (b) XRD patterns of fresh CuY zeolite with different loading [77]. Reprinted with permission from Ref. [77] copyright from Elsevier (Reprinted with permission from Ref. [58] copyright from Elsevier).

Table 7. Wavenumber, characteristics and functional group of catalyst.

Wavenumber (cm^{-1})	Characteristics and functional group	References
412-400, 597-615, 478	M-O	[228,229]
670	O-H	[229]
700-1300, 790	C-H bending vibration	[105,127]
875-750	C-H	[230]
919	N-O	[231]
1020, 1014	C-O stretching	[229]
1030	-OH	[232]
1051, 1117	Sulphate (SO_4^{2-})	[233]
1060	T-O (T= Si, Al)	[234]
1200, 1400	Si-O-Si	[235]
1211	C-O-C	[236]
1000-1450	C-O	[230]
1350	Stretching vibration of NO_3^-	[237]
1352	-NH	[238]
1384	C-N stretching	[229]
1396,1424-1429,1430	R-H, symmetric and asymmetric carboxyl group	[227,232,239]
1450	Benzene	[240]
1400,1650	H-OH bending vibration	[235]
1570	H-O-H absorption	[61]
1615-1580,1510-1450,1680-1620,1633,1515-1520,1571	C=C stretching	[229,230,233,236,240]
1635-1570	C=O	[241]
1618, 1563	Amide I and amide II	[242]
1630-1640, 1703	O-H bending vibration due to adsorbed water molecules at the catalyst surface	[227]
1647	C=N	[231]
1658, 1640-1650,1700,1680-1687	C=O	[230,237,243,244]
1731	Urethane	[242]
1739-1775	O-H stretching and bending vibration	[227]
2098	C≡N	[245]
2300	Isocyanate	[242]
2243	Nitrile	[231]
2800-3750	OH group	[235]
2839	Aliphatic C-H stretching vibration	[233]
2922, 3014, 2940,2924,2847,2925	Aromatic C-H stretching vibration	[105,232,233,246]
3400, 3420-3450, 3570, 3573-3574,3777,3430	O-H stretching and bending vibration	[61,105,227,232]
3700-3000	O-H, N-H, water molecule	[231,239]

nants using co-precipitation method for preparation of any catalyst [289]. Scherrer equation is used for determining the crystals size. Sometimes XRD pattern is also utilized for the quantitative investigation and detection purposes [218,219]. X-ray diffraction is not only used for the identification of structural change during phase transformation, but also to check the purity and improvement of catalyst (as shown in Figure 16 (a) [58]. Some studies reported that due to coating or burning of carbon nanotubes, peak decreases and get broad [139]. Broadening of peaks shows poor crystallinity and nonstructural dimensions [220]. Broadening or disappearing of peaks is due to the calcination of the sample. During calcination, catalyst is directly exposed to temperature and air, hence hydrolysis occurs and local sites gets affected. Few composites do show diffraction pattern or line which means that composite is in the amorphous state [221,222]. Due to the modification of catalyst, either by acid treatment, alkali treatment, heat treatment [58,118] or metal loading [77], diffraction pattern changes. Authors investigated that when copper loaded from 2.5 to 10 wt%, peaks decrease from 100% to 72% and less ordered structure are formed (as shown in Figure 16 (b) [77]. Holding time is not much more significant to change the crystal structure during calcination reported by Hu & co-researchers [118,223]. Any catalyst prepared by different methods (wet impregnation, hydrothermal method, etc.) can alter the structure of catalyst which can be observed by change in peaks [86]. XRD also reveals the impurities present in the catalyst or unreacted molecule. For calculation of particle size through XRD pattern, following formula (Williamson formula) can be used [224]:

$$\beta \cos\theta / \lambda = 1/L + \varepsilon \sin\theta / \lambda \quad (1)$$

where, β = full-width half maximum of diffraction peak, ε = strain, and L = crystalline size.

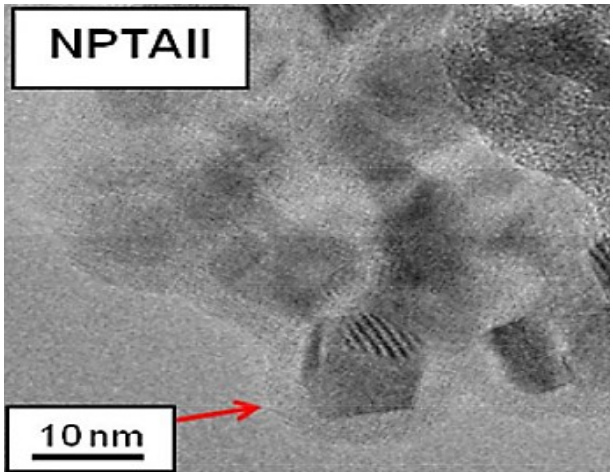

Figure 17. HRTEM image (Reprinted with permission from Ref. [253] copyright from Elsevier).

5.3 FTIR Analysis

The synthesized catalysts are examined using FTIR for the identification of interactions between the functional groups during catalyst preparation. Fourier transform infrared spectroscopy instrument is generally used to characterize the catalyst in terms of availability of functional groups like carboxyl (-COOH), a hydroxyl group (C-OH), epoxide (C-O-C), lactone etc. and associated chemical bonding [225,226]. In the investigation range functional group varies from wavenumber 400 to 4000 cm^{-1} [227]. FTIR value shows the bending or stretching of the bond between molecule or atoms. In present days, researchers use FTIR to analyze the peaks (broadening and narrowing of peaks) before and after the reaction to check the stability of catalyst [144]. The Table 7 shows the wavenumber and their respective functional groups.

5.4 TEM, HRTEM, STEM Analysis

Transmission Electron Microscopy (TEM) is used to elemental mapping, distribution or metallic dispersion of particle in the hybrid form of material. Uniform distribution of particle has significant catalytic efficiency [52,247]. TEM images are also used to determine the particle shape, size, and morphologies of particles [248-250]. High-Resolution Transmission Electron Microscopy (HRTEM) finds the microstructure and morphology of synthesized catalyst. HRTEM images reveal the extensive interface interaction between metal oxides like Fe_3O_4, Mn_3O_4, etc. [95,251]. It also differentiates the amorphous and crystal structure of particle (crystal is encapsulated with amorphous layer) as shown in the Figure 17 in red arrow [252]. Scanning transmission electron microscopy (STEM) shows the distribution of metal ions on support or matrix [253].

5.5 BET Analysis

BET (Brunauer-Emmett-Teller) analysis is used to study of the specific surface area of the catalyst. Different catalyst synthesis process could affect the characteristics and properties of the catalyst due to their varying surface area, i.e. it can control the catalytic behavior of

catalyst. The determination of surface area is directly related with the formation, deformation of bond or structure due to the thermal process, catalyst poisoning and also with catalytic performance. Catalytic activity will be high with higher surface area and with smaller pore volume [164]. Three methods are available to measure the surface area of any catalyst: volumetric, gravimetric, dynamic, but the commonly used method is the volumetric method based on nitrogen adsorption at fixed time and temperature [254]. With the analysis of BET, the total pore volume (p/p_0 = 0.98), average pore width (W=4.V_{mic}/S_{mic}) and the dia. of the catalyst using the Barrett-Joyner-Halenda (BJH) model can be determined [255].

5.6 Thermogravimetric Analysis (TGA)

Thermogravimetric Analysis (TGA) is conducted on powder to see the changes in weight with the changes in temperature. The changes in weight are correlated with the sample composition and stability. This analysis is extensively utilized to measure the thermal stability, composition, moisture, oxidative stability, volatile content, kinetics of decomposition, sample dehydration and lifetime. Schematic diagram of the TGA instrument is illustrated in Figure 18 [254]. Weight loss of the prepared catalyst in different temperature region is noted. Mostly, the first weight loss occurs at around 150 ^{o}C due to absorption of water molecules on the catalyst surface [164,283]. The weight loss above 500 ^{o}C is due to the oxidation loss [284,285].

5.7 Raman Spectroscopy

This instrument is used to know the crystal formation or ordered or disordered structure [256]. There are two important Raman peaks:

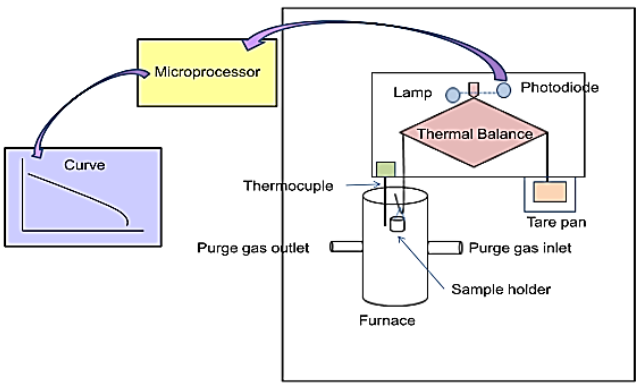

Figure 18. Schematic diagram of TGA instrument.

D band related to the disorders in the wall of catalyst and G band related to the C-C stretching mode of carbon, the intensity ratio of D and G band shows the degree of disorder in the walls of the catalyst [286-289]. An *et al.* used this technique to analyze the calcined catalyst (graphene -$BiFeO_3$) before and after the reaction and at the time of synthesis at 600 °C. Broadening and shifting of peaks in Raman Spectroscopy curve tells about the addition or doping of metal [150]. It is one of the popular vibrational spectroscope apart from FTIR which can be utilized to assess the motion of the molecule, identification of species and functional group [254].

5.8 Zeta Potential Measurement-Isoelectric Point (PZC- Point of Zero Charges)

Particle size distribution profile of suspended particles was determined using the dynamic light scattering (DLS) technique. The zeta potential indicates the degree of repulsion between adjacent charged particles in the dispersion and thus relate to the stability of the dispersion. At lower absolute zeta potential, particles get agglomerated, while resisting agglomeration at high absolute zeta potential. Zeta potential is used to determine the stability of catalyst at different pH. Zeta potential is nothing but a charge (in mV) present in the catalyst surface [257]. Zeta potential (ζ) and Isoelectric point (PZC) are related to each other. Zeta potential always decreases with the increase of pH. High zeta value of any catalyst means high stability. At low ζ, attraction exceeds repulsion and dispersion will break and flocculate [217]. Similar result was found by Cao *et al.* at pH of 10, low ζ value (-3.4) was obtained, but with the decreasing pH (pH from 3 to 9, the ζ values were 33.7mV, 25.5 mV, 18.9 mV, 4.52 mV, respectively), significant ζ value found [258]. According to Hogland *et al.* highest proportion of micropores have low ζ and PZC. This is due to the presence of high oxygen-containing functional groups [259]. An *et al.* reported that the catalyst activation ability decreases at high pH [256].

5.9 X-ray Photoelectron Spectroscopy (XPS)

XPS techniques are used to analyze the top surface layer and find the composition of material with electronic binding energy of prepared catalyst. The electron binding energy is calculated by the following formula:

$$E_k = h\upsilon - E_b - \Phi \quad (2)$$

where E_k is the kinetic energy of emitted photoelectron, hv is photo energy, Φ is work function, and E_b is binding energy.

The main advantages of XPS are to identify the chemical state on the surface and to differentiate the oxidation states of present molecules on the surface. It can identify the atomic concentration of O, C, S, and Fe on the catalyst surface. In Fenton process, the importance of XPS lies in the oxidation state of Fe on the catalyst surface which can be identified by this techniques and oxygen status also plays a vital role in oxidation process. There are four peaks under oxygen region, i.e. chemisorbed oxygen, lattice oxygen, chemically or physically adsorbed water. According to literature, chemisorbed oxygen plays an active role in oxidation process and increases the catalytic activity [46].

The binding energy is calculated only for the particular element [57,260]. Some researchers used XPS before and after the reaction and they found the regeneration of species and identified active species [21,258]. XPS results also validate the significant fabrication of catalyst [57].

5.10 Temperature Programmed Reduction Profiles (TPR)

TPR gives the knowledge about the nature of catalyst (reduction with temperature) when matrixed with supportive or other materials. This technique also gives the information about how any catalyst is formed/reduced in any composite surface with the varying percentage at a different temperature. Rezende *et al*. synthesized a catalyst of varying iron % with niobium and found the important information about iron reduction with temperature ($Fe_2O_3 \rightarrow Fe_3O_4 \rightarrow FeO \rightarrow Fe$ at different temperature 430 °C, 640 °C, 800 °C). They also revealed that the sample of 2.4% Fe/Nb at 600 °C with intensive peaks have excellent thermal stability and 7.6% Fe/Nb is more reactive [261].

5.11 Diffuse Reflectance Spectroscopy (DRS)

The UV-Vis DRS technology is used to find the band gap energy of any catalysts. It also reveals the UV and visible light absorption capacity of any catalyst when composites are coupled. The band gap decreases with increase in Fe concentration in the catalyst, it may be closer to pure Fe-oxide. An *et al*. found that graphene-$BiFeO_3$ (1.0 ev) have more light absorption capacity comparatively $BiFeO_3$ (2.05 ev) [256]. A similar investigation was done by some authors. They found that Fe_3O_4/g-C_3N_4 has high absorption capacity compared with g-C_3N_4 [262].

6. Application of Synthesized Catalyst in the Fenton Process

Main utilization of synthesized catalyst in the Fenton process is to treat synthetic and in-

Table 8. Application of synthesized catalyst in real wastewater.

Effluent type	Catalyst	Catalyst preparation method	Treatment/Removal/ Degradation				Ref.
			COD	Color	TOC	BOD	
Cosmetic industry	Fe/Al_2O_3 and Fe/AC	Incipient wetness impregnation method	85%	-	55%	-	[263]
Pharmaceutical industry	Fe-TiO_2	Dip coating method	83%	-	-	-	[264]
Household (sewage wastewater)	Fe/C	-	75%	-	-	-	[265]
Leather industry	MAC	-	69%		61%	74%	[266]
Fertilizer industry	Fe/TiO_2	Deposition-precipitation	-	-	96%	-	[267]
Oil refinery	Fe-pillared bentonite	ion exchange	92%	-	-	-	[268]
Pulp and Paper	Fe-Mn/NaY	Impregnation method/sol-gel	75.2%/ 45 %	-	-	-	[269]
Landfill leachates	GAC/Fe	Impregnation method	95%	93%	-	-	[270]
Textile industry	Fe/AC	Impregnation method	66.3%	96.7%	73.6%	72.5%	[271]

Table 9. Application of synthesized catalyst on dye effluent.

Dye	Catalyst	Catalyst preparation method	Degradation	Remark	Ref.
Methylene blue	$CoMoO_4$	Hydrothermal	100%	-High surface area= 61.9 m^2/g. -Universality.	[210]
Reactive Red 120	Fe-ZSM-5	Hydrothermal and Impregnation	98%	-High crystallinity, and surface area. -Reusable nano catalyst.	[272]
Basic violet 1 and Basic green 4	Cu-ZnO	Wet-Impregnation	95. 5% and 100%	-Promising sonophotocatalyst and excellent reusability.	[273]
RB-21, RR-141 and RG-6G	CZrW/ ZrW	Hydrothermal	95%, 92% and 50%	- CZrW is best found for degradation while ZrW was best for mineralization.	[274]
Reactive Blue 52	Fe-doped TiO_2	Microwave assisted hydrothermal	100%	>4 the release of iron in solution was found negligible.	[275]
Methyl Orange	NdFeB-AC	Negative pressure Impregnation method	97.8%	-Catalyst has good application prospect with high stability. -Catalytic degradation shows pseudo 1st order model.	[88]
Methyl green	CeCX	Impregnation	100%	-Catalyst show the synergetic effect (adsorption and oxidation)	[276]
Methylene Blue	Fe_3O_4/SiO_2/C nanoparticles (FSCNP)	Hydrothermal	94%	-Catalyst has large pH range, fast kinetics, good resistance against scavengers' radicals	[277]
Reactive Red 2	$CuFe_2O_4$	Co-precipitation	91.3%	-Catalyst show reusability, applicability and high stability. - NCFOH show high applicability than CFOH.	[100]
Rhodamine B	$Fe_2(MoO_4)_3$	Co-precipitation and sol gel	97%	-Synergistic effect of Fe^{3+} and MoO_4^{2-} $k_{co\text{-}precipitation}=1.5k_{solgel}$	[30]
Orange II	MeSrCuO	Sol gel	97%	-Cu^{2+} was active phase to degrade O II.	[278]
Methylene Blue	Kieselguhr/ Fe_2O_3/TiO_2	Co-precipitation and impregnation	98.86%	-Ecofriendly catalyst. -Easy recovery by external magnetic field.	[279]
Rhodamine B	Fe/SBA-15	Impregnation	93%	-Easily regenerated by soaking with H_2O_2. -Less leaching of iron and highly stable.	[280]
Methyl Orange and Rhodamine B	BaNaPW	Hydrothermal	>95%	-Bisfunction (photocatalyst and flocculant)	[99]
Methylene blue and Rhodamine B	Gr-Fe/Ce	Hydrothermal	>90%	-Ce plays a key role to lower the band gap.	[281]

dustrial wastewater. Currently, many types of wastewater are generated from various sectors that can be treated by Fenton process. Various researches already have been done with catalytic Fenton process, which are listed below in Table 8 and Table 9, represent the industrial wastewater contaminated with different dyes.

The evolution over the last two decades of heterogeneous catalyst preparation method, modification, characterization and overall application has been discussed. Heterogeneous catalysts have various advantages such as high surface area, less leaching of iron, less sludge formation, high recycling possibilities, ease in separation and faster rate of reaction which are useful for the suitable applications in the field of wastewater treatment using Fenton's process. The focus of this review is on the synthesis methods, physical and chemical modification to enhance their efficacy, factors which may possibly affect the performance of catalyst during synthesis, characterization such as SEM, XRD, TEM, PZC, TPR, DRS and applications.

The fundamentals of catalyst synthesis are extensively described in this review and the readers will get benefited from the deep insights. Among four synthesis methods, precipitation method was found to be most popular and used method based on Scopus data source.

The efficiency of catalyst can be enhanced by modification of catalyst and that modification is related to the changes in surface morphology and addition of foreign materials. Suitable shape and dimension of any synthesized catalyst is important to be effective catalyst. Diversified characteristics of catalyst can be achieved by only modification. Modification (doping) of catalyst enhances the morphological, magnetic, optical, structural and electrical properties. Small doping is not always fruitful for effective potential of catalyst at the same time. Ultrasound technique has a vital role to enhance the surface area of catalyst.

Low pH modified catalyst may have an excellent potential comparatively higher pH modified catalyst. It always enhances the catalytic efficiency. Calcination temperature may affect the characteristics and efficiency of catalyst. It also affects the reusability and hydrogenation of catalyst. High calcined catalyst have less surface area, loss of boding and uneven distribution compared to low calcined temperature. At low calcination temperature, catalyst becomes weak. Modifier could affect the structure, stability, activity and surface area of synthesized catalyst. Modifiers decrease the surface area but improves the activity and stability of catalyst.

The characterization methods, such as: SEM, XRD, FTIR, TEM, TGA, PZC, TPR, and DRS of synthesized catalyst, gives the ideas of their structure, nature, dimensions, shape, composition, functional group, distribution, dispersion, mapping, surface area, pore volume, diameter, thermal stability, nucleation, stability and band gap energy of catalyst.

7. Conclusion and Recommendations

The present review is focused on the different catalyst preparation methods like wet impregnation, hydrothermal, precipitation, and sol-gel. Different methods have their own significant importance, but the challenge is to identify the selectivity of the method. In this area, there is a tremendous hope to do something new by means of catalyst modification. Catalyst modification is a very vast area in the synthesis of the catalyst. The main objective of catalyst modification is to enhance the catalytic efficiency, fast catalytic reaction, surface area, pore volume, catalyst stability, and reusability. There are various ways to do modification on the catalyst, discussed in details in this review. Apart from established modification techniques, some new modification techniques need to be developed, so that it can be easily and cost-effectively applied in industrial scale level. In this work, we also discussed the factors which are responsible for the synthesis of effective catalysts like pH, temperature or modifier. Characterization of any catalyst is necessary to reveal the reason behind effective and successful catalyst. On the basis of that, we can optimize the synthesis method, modification techniques and other factors. Many characterizations already have been done by previous researchers, but in this work, only specific characterization was discussed for the synthesized catalyst.

Acknowledgment

This work was supported by Department of Science & Technology- Science & Engineering Research Board, File No. YSS/2014/000996, India.

References

[1] Guo, Y., Xue, Q., Zhang, H., Wang, N., Chang, S., Wang, H., Pang, H., Chen, H. (2018). *RSC Adv*., 8, 80–90.

[2] Soltani, T., Lee, B.K., Hazard, J. (2016). *Mater*., 316, 122–133.

[3] Ashokkumar, M., Cavalieri, F., Chemat, F., Okitsu, K., Sambandam, A., Yasui, K., Zisu, B. (2016). *Handbook of Ultrasonics and Sonochemistry*.

[4] Banerjee, S., Benjwal, P., Singh, M., Kar, K.K. (2018). *Appl. Surf. Sci.,* 439, 560–568.

[5] Diya'uddeen, B.H., Rahim Pouran, S., Abdul Aziz, A.R., Daud, W.M.A.W. (2015). *RSC Adv*., 5, 68159–68168.

[6] Zhuang, H., Shan, S., Fang, C., Song, Y., Xue, X. (2018). *Bioresources*, 13, 4175–4186.

[7] Song, Y., Rong, C., Shang, J., Wang, Y., Zhang, Y., Yu, K. (2017). *J. Chem. Technol. Biotechnol*., 92, 2038–2049.

[8] Ogbiye, A.S., Omole, D.O., Ade-Balogun, K.D., Onakunle, O., Elemile, O.O. (2018). *Cogent. Eng.,* 5, 1–15.

[9] Asaithambi, P., Matheswaran, M. (2016). *Arab. J. Chem.,* 9, S981–S987.

[10] Carrasco-Díaz, M.R., Castillejos-López, E., Cerpa-Naranjo, A., Rojas-Cervantes, M.L. (2017). *Microporous Mesoporous Mater*., 237, 282–293.

[11] Ternes, T.A. (1998). *Water Res*., 32, 3245–3260.

[12] Du, D., Shi, W., Wang, L., Zhang, J. (2017). *Appl. Catal. B Environ*., 200, 484–492.

[13] Lima, M.J., Silva, C.G., Silva, A.M.T., Lopes, J.C.B., Dias, M.M., Faria, J.L. (2017). *Chem. Eng. J.,* 310, 342–351.

[14] Sun, X., Wang, C., Li, Y., Wang, W., Wei, J. (2015). *Desalination,* 355, 68–74.

[15] Mohammadi, S., Kargari, A., Sanaeepur, H., Abbassian, K., Najafi, A., Mofarrah, E. (2015). *Desalin. Water Treat*., 53, 2215–2234.

[16] Villegas, L.G.C., Mashhadi, N., Chen, M., Mukherjee, D., Taylor, K.E., Biswas, N. (2016). *Curr. Pollut. Reports,* 2, 157–167.

[17] Dang, T.H., Denat, A. (2018). 2nd International conference on advanced materials (ICAM-2017), *IOP Conf. Series: Mater. Sci. Eng*., 305, 1-10

[18] Gao, P., Song, Y., Hao, M., Zhu, A., Yang, H., Yang, S. (2018). *Sep. Purif. Technol*., 201, 238–243.

[19] Gupta, D., Garg, A., (2018). *React. Kinet. Mech. Catal*., 124, 101–121.

[20] Chen, W., Yang, X., Huang, J., Zhu, Y., Zhou, Y., Yao, Y., Li, C. (2016). *Electrochim. Acta,* 200, 75–83.

[21] Sheng, Y., Sun, Y., Xu, J., Zhang, J., Han, Y.F. (2018). *AIChE J*., 64, 538–549.

[22] Vasilyeva, M.S., Rudnev, V.S., Zvereva, A.A., Ustinov, A.Y., Arefieva, O.D., Kuryavyi, V.G., Zverev, G.A. (2018). *J. Photochem. Photobiol. A Chem*., 356, 38–45.

[23] Dinarvand, M., Sohrabi, M., Royaee, S.J., Zeynali, V. (2017). *Asia-Pacific J. Chem. Eng*., 12, 631–639.

[24] Duan, F., Yang, Y., Li, Y., Cao, H., Wang, Y., Zhang, Y. (2014). *J. Environ. Sci. (China),* 26, 1171–1179.

[25] Nagabhushana, H., Saundalkar, S.S., Muralidhar, L., Nagabhushana, B.M. (2011). *Chinese Chem. Lett*., 22, 143–146.

[26] Wang, W.M., Song, J., Han, X. (2013). *J. Hazard. Mater*., 262, 412–419.

[27] Yu, L., Chen, J., Liang, Z., Xu, W., Chen, L., Ye, D. (2016). *Sep. Purif. Technol*., 171, 80–87.

[28] Jinisha, R., Gandhimathi, R., Ramesh, S.T., Nidheesh, P.V., Velmathi, S. (2018). *Chemospherem,* 200, 446–454.

[29] Rostamizadeh, M., Jafarizad, A., Gharibian, S. (2018). *Sep. Purif. Technol*., 192, 340–347.

[30] Rashad, M.M., Ibrahim, A.A., Rayan, D.A., Sanad, M.M.S., Helmy, I.M. (2017). *Environ. Nanotechnology, Monit. Manag*., 8, 175–186.

[31] Muruganandam, L., Kumar, M.P.S., Jena, A., Gulla, S., Godhwani, B. (2017). *IOP Conf. Ser. Mater. Sci. Eng*., 263, 1-11.

[32] Sowinska, A., Pawlak, M., Mazurkiewicz, J., Pacholska, M. (2017). *Water (Switzerland),* 9, 1–14.

[33] A.R. Martins, A.B. Salviano, A.A.S. Oliveira, R. V. Mambrini, F.C.C. Moura, (2017) *Environ. Sci. Pollut. Res*. 24, 5991–6001.

[34] A. Jain, M. Kotwal, S. Khan, 1 (2016) Asian *J. Chem. Pharm. Sci.* 1–22.

[35] S. Krishnan, H. Rawindran, C.M. Sinnathambi, J.W. Lim, (2017) *IOP Conf. Ser. Mater. Sci. Eng.* 206, 1-11.

[36] M. Baerns (2004). *Series: Springer Series in Chemical Physics*, 75, 6221-6779.

[37] Alam, U., Khan, A., Bahnemann, D., Muneer, M. (2018). *J. Colloid Interface Sci*., 509, 68–72.

[38] Chanderia, K., Kumar, S., Sharma, J., Ameta, R., Punjabi, P.B. (2017). *Arab. J. Chem*., 10, S205–S211.

[39] Córdoba, A., Saux, C., Pierella, L.B. (2017). *Appl. Catal. A Gen*., 544, 173–180.

[40] Dong, Q., Chen, Y., Wang, L., Ai, S., Ding, H. (2017). *Appl. Surf. Sci*., 426, 1133–1140.

[41] Karthikeyan, S., Pachamuthu, M.P., Isaacs, M.A., Kumar, S., Lee, A.F., Sekaran, G. (2016). *Appl. Catal. B Environ*., 199, 323–330.

[42] Lan, H., Wang, A., Liu, R., Liu, H., Qu, J. (2015). *J. Hazard. Mater*., 285, 167–172.

[43] Guo, S., Zhang, G., Guo, Y., Yu, J.C. (2013). *Carbon*, 60, 437–444.

[44] Wei, G.T., Fan, C.Y., Zhang, L.Y., Ye, R.C., Wei, T.Y., Tong, Z.F. (2012). *Catal. Commun.,* 17, 184–188.

[45] Pachamuthu, M.P., Karthikeyan, S., Maheswari, R., Lee, A.F., Ramanathan, A. (2017). *Appl. Surf. Sci.*, 393, 67–73.

[46] Liu, T., You, H., Chen, Q. (2009). *J. Hazard. Mater*., 162, 860–865.

[47] Noorjahan, M., Durga Kumari, V., Subrahmanyam, M., Panda, L. (2005). *Appl. Catal. B Environ*., 57, 291–298.

[48] Araña, J., González Díaz, O., Doña Rodríguez, J.M., Herrera Melián, J.A., Garriga i Cabo, C., Pérez Peña, J., Carmen Hidalgo, M., Navío-Santos, J.A. (2003). *J. Mol. Catal. A Chem*., 197, 157–171.

[49] Zhao, D., Yi, B.L., Zhang, H.M., Yu, H.M., Wang, L., Ma, Y.W., Xing, D.M. (2009). *J. Power Sources,* 190, 301–306.

[50] Dükkancı, M., Gündüz, G., Yılmaz, S., Prihod, R.V., Dükkanci, M, Gündüz, G., Yilmaz, S., Prihod'ko, R.V. (2010). *J. Hazard. Mater*., 181, 343–350.

[51] Gajović, A., Silva, A.M.T., Segundo, R.A., Šturm, S., Jančar, B., Čeh, M. (2011). *Appl. Catal. B Environ*., 103, 351–361.

[52] Wu, M., Yan, J.M., Zhao, M., Jiang, Q. (2012). *Chempluschem,* 77, 931–935.

[53] Chen, Y., Li, N., Zhang, Y., Zhang, L. (2014). *J. Colloid Interface Sci*., 422, 9–15.

[54] Zhang, X., Zhang, Y., Gao, L., Yu, H., Wei, Y. (2015). *J. Colloid Interface Sci*., 452, 24–32.

[55] An, J, Zhang, G., Zheng, R., Wang, P. (2016). *J. Environ. Sci. (China),* 48, 218–229.

[56] Han, C., Huang, G., Zhu, D., Hu, K. (2017). *Mater. Chem. Phys*., 200, 16–22.

[57] Bian, L., Liu, Y., Zhu, G., Yan, C., Zhang, J., Yuan, A. (2018). *Ceram. Int*., 44, 7580–7587.

[58] Diao, Y., Yan, Z., Guo, M., Wang, X. (2018). *J. Hazard. Mater*., 344, 829–838.

[59] He, Y., Bin Jiang, D., Jiang, D.Y., Chen, J., Zhang, Y.X. (2018). *J. Hazard. Mater*., 344, 230–240.

[60] Escribano, P.G., del Río, C., Morales, E., Aparicio, M., Mosa, J. (2018). *J. Memb. Sci*., 551, 136–144.

[61] Vinosha, P.A., Das, S.J., Annie Vinosha, P., Jerome Das, S. (2018). *Mater. Today Proc*., 5, 8662–8671.

[62] Rezgui, S., Amrane, A., Fourcade, F., Assadi, A., Monser, L., Adhoum, N. (2018). *Appl. Catal. B Environ*. 226, 346–359.

[63] Sharma, A., Dutta, R.K. (2018). *J. Clean. Prod*., 185, 464–475.

[64] García, J.C., Castellanos, M.P., Uscátegui, Á., Fernández, J., Pedroza, A.M., Daza, C.E. (2012). *Univ. Sci*., 17, 303–314.

[65] Ayoub, H., Roques-Carmes, T., Potier, O., Koubaissy, B., Pontvianne, S., Lenouvel, A., Guignard, C., Mousset, E., Poirot, H., Toufaily, J., Hamieh, T. (2018). Environ. *Sci. Pollut. Res.*, 25, 34950-34967 .

[66] Wang, N. (2017). *RSC Adv.*, 7, 27619–27628.

[67] Mostafa Sadek, A. (2016). *Am. J. Chem. Eng*., 4, 1-8.

[68] Wang, N., Chen, J., Zhao, Q., Xu, H. (2017). *RSC Adv*., 7, 52524–52532.

[69] Wang, N., Hao, L., Chen, J., Zhao, Q., Xu, H. (2018). *Environ. Sci. Pollut. Res*., 25, 12481-12490.

[70] Barbosa, I.A., Zanatta, L.D., Espimpolo, D.M., da Silva, D.L., Nascimento, L.F., Zanardi, F.B., de Sousa Filho, P.C., Serra, O.A., Iamamoto, Y. (2017). *Solid State Sci*., 72,14–20.

[71] Mena, I.F., Diaz, E., Rodriguez, J.J., Mohedano, A.F. (2017). *Chem. Eng. J*., 318, 153–160.

[72] Garrido-Ramírez, E.G., Marco, J.F., Escalona, N., Ureta-Zañartu, M.S. (2016). *Microporous Mesoporous Mater*., 225, 303–311.

[73] Idrissi, M., Miyah, Y., Benjelloun, Y., Chaouch, M. (2016). *J. Mater. Environ. Sci*., 7, 50–58.

[74] Doumic, L.I., Salierno, G., Ramos, C., Haure, P.M., Cassanello, M.C., Ayude, M.A. (2016). *RSC Adv*., 6, 46625–46633.

[75] Esteves, B.M., Rodrigues, C.S.D., Boaventura, R.A.R., Maldonado-Hódar, F.J., Madeira, L.M. (2016). *J. Environ. Manage*., 166, 193–203.

[76] Zhang, R., You, H., Wu, D. (2016). *Desalin. Water Treat.*, 57, 12010–12018.

[77] Singh, L., Rekha, P., Chand, S. (2016). *Sep. Purif. Technol.*, 170, 321–336.

[78] Sable, S.S., Ghute, P.P., Álvarez, P., Beltrán, F.J., Medina, F., Contreras, S. (2015). *Catal. Today,* 240, 46–54.

[79] di Luca, C., Ivorra, F., Massa, P., Fenoglio, R. (2015). *Chem. Eng. J.*, 268, 280–289.

[80] Lu, M., Yao, Y., Gao, L., Mo, D., Lin, F., Lu, S. (2015). *Water. Air. Soil Pollut.*, 226, 87-90.

[81] Pan, W., Zhang, G., Zheng, T., Wang, P. (2015). *RSC Adv.*, 5, 27043–27051.

[82] Xie, F., Zhong, J., Wang, L., Wang, K., Hua, D.X. (2015). *IOP Conf. Ser. Mater. Sci. Eng.*, 87, 1-7.

[83] Ersöz, G. (2014). *Appl. Catal. B Environ.*, 147, 353–358.

[84] Zaidill Azizan, M.A., Hassan, H., Faraziehan, S., Abu Hassan, N. (2014). *Appl. Mech. Mater.*, 661, 29–33.

[85] Xiong, W., Liu, D.R., Yuan, G.Y., Wei, Q., Sen Dang, Q., Feng, J., Xu, B. (2014). *Adv. Mater. Res.*, 881–883, 279–282.

[86] Ramli, R.M., Kait, C.F., Omar, A.A. (2014). *Adv. Mater. Res.*, 917, 160–167.

[87] Azmi, N.H.M., Vadivelu, V.M., Hameed, B.H. (2014). *Desalin. Water Treat.*, 52, 5583–5593.

[88] Yang, C., Wang, D., Tang, Q. (2014). *J. Taiwan Inst. Chem. Eng.*, 45, 2584–2589.

[89] Bayat, M., Sohrabi, M., Royaee, S.J. (2012). *J. Ind. Eng. Chem.*, 18, 957–962.

[90] Xu, J.Q., Guo, F., Zou, S.S., Quan, X.J. (2011). *Mater. Sci. Forum,* 694, 640–644.

[91] Xu, L., Wang, J. (2012). *Environ. Sci. Technol.*, 46, 10145–10153.

[92] Dhaouadi, A., Adhoum, N. (2010). *Appl. Catal. B Environ.*, 97, 227–235.

[93] Shukla, P., Wang, S., Sun, H., Ang, H.M., Tadé, M. (2010). *Chem. Eng. J.*, 164, 255–260.

[94] Gan, G., Liu, J., Zhu, Z., Yang, Z., Zhang, C., Hou, X. (2017). *Chemosphere,* 168, 254–263.

[95] Wan, Z., Wang, J. (2017). *J. Hazard. Mater.*, 324, 653–664.

[96] Jusoh, R., Jalil, A.A., Triwahyono, S., Idris, A., Noordin, M.Y. (2015). *Sep. Purif. Technol.*, 149, 55–64.

[97] Haber, J., Block, J., H., Delmon, B. (1995). *Pure Appl. Chem.*, 67, 1257-1306.

[98] Bian, L., Liu, Y., Zhu, G., Yan, C., Zhang, J., Yuan, A. (2018). *Ceram. Int.*, 44, 7580-7587.

[99] Fei, B.L., Zhong, J.K., Deng, N.P., Wang, J.H., Liu, Q.B., Li, Y.G., Mei, X. (2018). *Chemosphere,* 197, 241–250.

[100] Yu, D., Ni, H., Wang, L., Wu, M., Yang, X. (2018). *J. Clean. Prod.*, 186, 146–154.

[101] Xiao, C., Li, J., Zhang, G. (2018). J. *Clean. Prod.*, 180, 550–559.

[102] Edla, R., Tonezzer, A., Orlandi, M., Patel, N., Fernandes, R., Bazzanella, N., Date, K., Kothari, D.C., Miotello, A. (2017). *Appl. Catal. B Environ.*, 219, 401–411.

[103] Jaramillo-Páez, C., Navío, J.A., Hidalgo, M.C., Bouziani, A., El Azzouzi, M. (2017). *J. Photochem. Photobiol. A Chem.*, 332, 521–533.

[104] Zhao, Z., Zhou, X., Liu, Z. (2015). *Water Air Soil Pollut.*, 228, 463, 1-11.

[105] Liang, C., Liu, Y., Li, K., Wen, J., Xing, S, Ma, Z., Wu, Y. (2017). *Sep. Purif. Technol.*, 188, 105–111.

[106] Ma, P., Yu, Y., Xie, J., Fu, Z. (2017). *Adv. Powder Technol.*, 28, 2797–2804.

[107] Ojha, D.P., Joshi, M.K., Kim, H.J. (2017). *Ceram. Int.*, 43, 1290–1297.

[108] To, T., Phan, N., Nikoloski, A.N., Bahri, P.A., Li, D. (2017). *RSC. Adv.*, 8, 36181-36190.

[109] Sun, H., Dong, B., Song, L., Du, J., Gao, R., Su, G., Cao, L. (2017). *J. Photochem. Photobiol. A Chem.*, 334, 20–25.

[110] Dhiman, M., Sharma, R., Kumar, V., Singhal, S. (2016). *Ceram. Int.*, 42, 12594–12605.

[111] Wang, Z., Fan, Y., Wu, R., Huo, Y., Wu, H., Wang, F., Xu, X. (2018). *RSC Adv.*, 8, 5180–5188.

[112] Turki, A., Kochkar, H., Berhault, G., Ghorbel, A., (2010). *P-Hydroxybenzoic Acid Degradation by Fe/Pd-HNT Catalysts with in Situ Generated Hydrogen Peroxide*, Elsevier B.V.

[113] Wu, D., Long, M., Chen, C., Wu, Y., Cai, W., Zhou, J., Ding, D. (2009). *Water Sci. Technol.*, 59, 565–571.

[114] Bolova, E., Gunduz, G., Dukkanci, M., Yilmaz, S., Yaman, Y.C. (2011). *Int. J. Chem. React. Eng.*, 9, 1-20.

[115] Li, D., Pan, C., Shi, R., Zhu, Y. (2011). *CrystEngComm,* 13, 6688.

[116] Xu, Z., Zhang, M., Wu, J., Liang, J., Zhou, L., Lü, B. (2013). *Water Sci. Technol.*, 68, 2178–2185.

[117] Vu, T.A., Le, G.H., Dao, C.D., Dang, L.Q., Nguyen, K.T., Dang, P.T., Tran, H.T.K., Duong, Q.T., Nguyen, T.V., Lee, G.D. (2014). *RSC Adv.*, 4, 41185–41194.

[118] Hu, Z.T., Da Oh, W., Liu, Y., Yang, E.H., Lim, T.T. (2018). *J. Colloid Interface Sci*., 509, 502–514.

[119] Ren, M., Qian, X., Fang, M., Yue, D., Zhao, Y. (2018). *Res. Chem. Intermed*., 44, 4103-4117.

[120] Ridruejo, C., Alcaide, F., Álvarez, G., Brillas, E., Sirés, I. (2018). *J. Electroanal. Chem*., 808, 364–371.

[121] Zhang, X., Dong, J., Hao, Z., Cai, W., Wang, F. (2018). *Trans. Tianjin Univ*., 24, 361-369.

[122] Zhang, H., Xue, G., Chen, H., Li, X. (2018). *Chemosphere,* 191, 64–71.

[123] Zhang, Z., Guo, Y., Wang, Q., Louis, B., Qi, F. (2017). *Comptes Rendus Chim*., 20, 87–95.

[124] Zhang, L., Xu, D., Hu, C., Shi, Y. (2017). *Appl. Catal. B Environ*., 207, 9–16.

[125] Xie, Z., Wang, C., Yin, L. (2017). *J. Catal*., 353, 11–18.

[126] Wang, X., Dou, L., Yang, L., Yu, J., Ding, B. (2017). *J. Hazard. Mater*., 324, 203–212.

[127] Tang, J., Wang, J. (2017). *RSC Adv*., 7, 50829–50837.

[128] Ramesh, M., Rao, M.P., Rossignol, F., Nagaraja, H.S. (2017). *Water Sci. Technol*., 76, 1652-1665.

[129] Kim, E.J., Oh, D., Lee, C.S., Gong, J., Kim, J., Chang, Y.S. (2017). *Catal. Today,* 282, 71–76.

[130] Li, J, Zhang, S., Chen, Y., Liu, T., Liu, C., Zhang, X., Yi, M., Chu, Z., Han, X. (2017). *RSC Adv*., 7, 29051–29057.

[131] Chai, F., Li, K., Song, C., Guo, X. (2016). *J. Colloid Interface Sci*., 475, 119–125.

[132] Li, S., Zhang, G., Zhang, W., Zheng, H., Zhu, W, Sun, N., Zheng, Y., Wang, P. (2017). *Chem. Eng. J*., 326, 756–764.

[133] Li, S., Zhang, G., Zheng, H., Wang, N., Zheng, Y., Wang, P. (2016). *RSC Adv*., 6, 82439–82446.

[134] Wang, R., Liu, X., Wu, R., Yu, B., Li, H., Zhang, X., Xie, J., Yang, S.-T. (2016). *RSC Adv*., 6, 8594–8600.

[135] Yang, X., Sun, H., Zhang, L., Zhao, L., Lian, J., Jiang, Q. (2016). *Sci. Rep*., 6, 1–12.

[136] Mao, Y., Zou, H., Wang, Q., Huang, C. (2016). *Sci. China Chem*., 59, 903–909.

[137] Lyu, L., Zhang, L., Hu, C., Yang, M. (2016). *J. Mater. Chem. A,* 4, 8610–8619.

[138] Kong, L., Zhou, X., Yao, Y., Jian, P., Diao, G. (2016). *Environ. Technol. (United Kingdom),* 37, 422–429.

[139] Hao, S.M., Qu, J., Zhu, Z.S., Zhang, X.Y., Wang, Q.Q., Yu, Z.Z. (2016). *Adv. Funct. Mater*., 26, 7334–7342.

[140] Fang, D., Yu, Y., Xu, Z., Liang, J, Zhou, L. (2016). *Mater. Chem. Phys*., 171, 386-393.

[141] Zhou, M., Li, W., Du, Y., Kong, D., Wang, Z., Meng, Y., Sun, X., Yan, T., Kong, D., You, J. (2016). *J. Nanoparticle Res*.,18, 346, 1-15.

[142] Lyu, L., Zhang, L., Hu, C. (2016). *Environ. Sci. Nano,* 3, 1483–1492.

[143] Edla, R., Patel, N., Orlandi, M., Bazzanella, N., Bello, V., Maurizio, C., Mattei, G., Mazzoldi, P., Miotello, A. (2015). *Appl. Catal. B Environ*., 166–167, 475–484.

[144] Jia, Y., Wu, C., Kim, D.H, Lee, B.W., Rhee, S.J., Park, Y.C., Kim, C.S., Wang, Q.J., Liu, C. (2018). *Chem. Eng. J*., 337, 709–721.

[145] Mahy, J.G, Tasseroul, L., Herlitschke, M., Hermann, R.P., Lambert, S.D. (2016). *Mater. Today Proc*., 3, 464–469.

[146] Uma, K., Arjun, N., Pan, G.T., Yang, T.C.K. (2017). *Appl. Surf. Sci*., 425, 377–383.

[147] Nurhayati, E., Yang, H., Chen, C., Liu, C., Juang, Y., Huang, C., chang Hu, C. (2016). *Int. J. Electrochem. Sci*., 11, 3615–3632.

[148] Wang, L., Yu, Z., Peng, Z., Chen, Y., Xiang, G., Liu, Q., Liu, Y., Chen, D. (2016). *Russ. J. Phys. Chem. A,* 90, 777–782.

[149] Martínez, F., Molina, R., Pariente, M.I., Siles, J.A, Melero, J.A. (2017). *Catal. Today,* 280, 176–183.

[150] Soltani, T., Lee, B.K. (2017). *Chem. Eng. J*., 313, 1258–1268.

[151] Su, L, Li, K., Zhang, H., Fan, M., Ying, D., Sun, T., Wang, Y., Jia, J. (2017). *Water Res*., 120, 1–11.

[152] Ribeiro, R.S., Frontistis, Z., Mantzavinos, D., Venieri, D., Antonopoulou, M., Konstantinou, I., Silva, A.M.T., Faria, J.L., Gomes, H.T. (2016). *Appl. Catal. B Environ*., 199, 170–186.

[153] Soltani, T., Lee, B.K. (2016). *J. Mol. Catal. A Chem*., 425, 199–207.

[154] Cheng, C.K., Kong, Z.Y., Khan, M.R. (2015). *Water. Air. Soil Pollut*., 226, 1-12.

[155] Feng, J., Wong, R.S.K., Hu, X., Yue, P.L. (2004). *Catal. Today,* 98, 441–446.

[156] Vinosha, P.A., Xavier, B., Krishnan, S., Das, S.J. (2018). *Mater. Res. Bull*., 101, 190–198.

[157] Vinosha, P.A., Xavier, B., Anceila, D., Das, S.J. (2018). *Optik (Stuttg)*, 157, 441–448.

[158] Vinosha, P.A., Xavier, B., Ashwini, A., Ansel Mely, L., Das, S.J. (2017). *Optik (Stuttg).,* 137, 244–253.

[159] Xu, H.-Y., Wang, Y., Shi, T.-N., Zhao, H., Tan, Q., Zhao, B.-C., He, X.-L., Qi, S.-Y. (2018). *Front. Mater. Sci*., 12, 34–44.

[160] Zuorro, A., Lavecchia, R., Monaco, M.M., Iervolino, G., Vaiano, V. (2017). *Catalysts*, 9(8), 645.

[161] Bai, J., Liu, Y., Yin, X., Duan, H., Ma, J. (2017). *Appl. Surf. Sci*., 416, 45–50.

[162] Barbosa, I.A., Zanatta, L.D., Espimpolo, D.M., da Silva, D.L., Nascimento, L.F., Zanardi, F.B., de Sousa Filho, P.C., Serra, O.A., Iamamoto, Y. (2017). *Solid State Sci*., 72, 14–20.

[163] Fida, H., Zhang, G., Guo, S., Naeem, A. (2017). *J. Colloid Interface Sci*., 490, 859–868.

[164] Gogoi, A., Navgire, M., Sarma, K.C., Gogoi, P. (2017). *Chem. Eng. J*., 311, 153–162.

[165] Liu, Y., Zhang, G., Chong, S., Zhang, N., Chang, H., Huang, T., Fang, S. (2017). *J. Environ. Manage*., 192, 150–155.

[166] Shen, Y., Zhou, Y., Zhang, Z., Xiao, K. (2017). *J. Ind. Eng. Chem*., 52, 153–161.

[167] Tian, X., Liu, Y., Chi, W., Wang, Y., Yue, X., Huang, Q., Yu, C. (2017). *Water. Air. Soil Pollut.,* 228, 1-12.

[168] Wan, D., Wang, G., Li, W., Wei, X. (2017). *Appl. Surf. Sci*., 413, 398–407.

[169] Ya, V., Martin, N., Chou, Y.H., Chen, Y.M., Choo, K.H., Chen, S.S., Li, C.W. (2018). *J. Taiwan Inst. Chem. Eng*., 83, 107–114.

[170] Xu, R., Huang, X., Li, H., Su, M., Chen, D. (2018). *IOP Conf. Ser. Earth Environ. Sci*., 111, 1-6.

[171] Tiya-Djowe, A., Ruth, N., Kamgang-Youbi, G., Acayanka, E., Laminsi, S., Gaigneaux, E.M. (2018). *Microporous Mesoporous Mater*., 255, 148–155.

[172] Shi, X., Tian, A., You, J., Yang, H., Wang, Y., Xue, X. (2018). *J. Hazard. Mater*., 353, 182–189.

[173] Santos, A.P.F., Souza, B.M., Silva, T.F.C.V., Cavalcante, R.P., Oliveira, S.C., Machulek, A., Boaventura, R.A.R., Vilar, V.J.P. (2018). *Environ. Sci. Pollut. Res*., 25, 1–13.

[174] He, H., Zhang, X., Yang, C., Zeng, G., Li, H., Chen, Y. (2018). *J. Environ. Eng*., 144, 04018041.

[175] Zhang, H., Liu, J., Ou, C., Faheem, C., Shen, J., Yu, H.., Jiao, Z., Han, W., Sun, X., Li, J., Wang, L. (2017). *J. Environ. Sci. (China).* 53, 1–8.

[176] Takayanagi, A., Kobayashi, M., Kawase, Y. (2017). *Environ. Sci. Pollut. Res*., 24, 8087–8097.

[177] Vilar, V.J.P., Silva, T.F.C.V., Santos, M.A.N., Fonseca, A., Saraiva, I., Boaventura, R.A.R. (2012). *Sol. Energy,* 86, 3301–3315.

[178] Nogueira, A.A., Souza, B.M., Dezotti, M.W.C., Boaventura, R.A.R., Vilar, V.J.P. (2017). *J. Photochem. Photobiol. A Chem*., 345, 109–123.

[179] Glugoski, L.P., de Jesus Cubas, P., Fujiwara, S.T. (2017). *Environ. Sci. Pollut. Res*. 24, 6143–6150.

[180] Frade, V.M.F., Converti, A., Al Arni, S., Silva, M.F., Palma, M.S.A. (2017). *Chem. Eng. Technol*., 40, 663–669.

[181] Emin, M., Alver, A, Karataş, M. (2017). *Journal name??*, 90, 21241.

[182] Xie, X., Hu, Y., Cheng, H. (2016). *Water Res*., 89, 59–67.

[183] Wang, P., Wang, L., Sun, Q., Qiu, S., Liu, Y., Zhang, X, Liu, X., Zheng, L. (2016). *Mater. Lett*., 183, 61–64.

[184] Valero-Luna, C., Palomares-Sanchéz, S.A., Ruíz, F. (2016). *Catal. Today,* 266, 110–119.

[185] Su, C., Li, W., Liu, X., Huang, X., Yu, X. (2016). *Front. Environ. Sci. Eng*., 10, 37–45.

[186] Peng, S., Zhang, W., He, J., Yang, X., Wang, D., Zeng, G. (2016). *J. Environ. Sci. (China),* 41, 16–23.

[187] Expósito, A.J., Monteagudo, J.M., Díaz, I., Durán, A. (2016). *Chem. Eng. J*., 306, 1203–1211.

[188] W., Wan, D., Wang, G., Chen, K., Hu, Q., Lu, L. (2016). *Korean J. Chem. Eng*., 33, 1557–1564.

[189] Kim Phuong, N.T., wook Beak, M., Huy, B.T., Lee, Y.I. (2016). *Chemosphere,* 146, 51–59.

[190] Nadejde, C., Neamtu, M., Hodoroaba, V.D., Schneider, R.J., Paul, A., Ababei, G., Panne, U. (2015). *J. Nanoparticle Res*., 17, 1–10.

[191] Ealias, A.M., Jose, J.V., Saravanakumar, M.P. (2016). *Environ. Sci. Pollut. Res*., 23, 21416–21430.

[192] Kakarla, P.K., Andrews, T., Greenberg, R.S., Zervas, D.S. (2002). *Remediation,* 12, 23–36.

[193] Reyes, I.A., Patiño, F., Flores, M.U., Narayanan, J., Calderón, H., Pandiyan, T. (2013). *J. Mex. Chem. Soc*., 57, 96–104.

[194] Barbusiński, K. (2014). *Polish J. Environ. Stud.* 14(3), 281-285.

[195] Banuelos, J.A., Garcia-Rodriguez, O., Rodriguez-Valadez, F.J., Godinez, L.A. (2015). *J. Electrochem. Soc*., 162, E154–E159.

[196] Rahman, W.U., Khan, M.D., Khan, M.Z., Halder, G. (2018). *J. Environ. Chem. Eng*., 6, 2957–2964.

[197] Ganesan, R., Thanasekaran, K. (2011). *Int. J. Environ. Sci*., 1, 1168–1176.

[198] Lewis, S., Lynch, A., Bachas, L., Hampson, S., Ormsbee, L., Bhattacharyya, D. (2009). *Environ. Eng. Sci.*, 26, 849–859.

[199] Lee, S., Oh, J., Park, Y. (2006). *Bull. Chem. Soc.*, 27, 489–494.

[200] Zhao, X., Dong, Y., Cheng, B., Kang, W. (2013). *Int. J. Photoenergy,* 2009, 1-9.

[201] Pradisty, N.A., Sihombing, R., Howe, R.F., Krisnandi, Y.K. (2017). *Makara J. Sci.*, 21, 25–33.

[202] Tony, M.A., Zhao, Y.Q., Purcell, P.J., El-Sherbiny, M.F. (2009). *J. Environ. Sci. Heal. - Part A Toxic/Hazardous Subst. Environ. Eng.*, 44, 488–493.

[203] Lee, S.Y., Park, S.J. (2013). *J. Ind. Eng. Chem.*, 19, 1761–1769.

[204] Kurian, M., Nair, D.S. (2015). *J. Water Process Eng.*, 8, e37–e49.

[205] Lee, H., Choi, J., Lee, S., Yun, S.T., Lee, C., Lee, J. (2013). *Appl. Catal. B Environ.*, 138–139, 311–317.

[206] Huang, Z., Wu, P., Li, H., Li, W., Zhu, Y., Zhu, N. (2014). *RSC Adv.*, 4, 6500.

[207] Liang, C., Zhao, W., Song, Z., Xing, S. (2017). *RSC Adv.*, 7, 35257–35264.

[208] Huang, H., Shan, W., Yang, S., Zhang, J. (2014). *Catal. Sci. Technol.*, 4, 3611–3614.

[209] Yong, E.L., Lin, Y.P. (2016). *RSC Adv.*, 6, 18587–18595.

[210] Fan, Y., Ma, W., He, J., Du, Y. (2017). *RSC Adv.*, 7, 36193–36200.

[211] Chen, Y.F., Lee, C.Y., Yeng, M.Y., Chiu, H.T. (2003). *J. Cryst. Growth,* 247, 363–370.

[212] Li, G., Liu, Z.Q., Lu, J., Wang, L., Zhang, Z. (2009). *Appl. Surf. Sci.*, 255, 7323–7328.

[213] Park, G.C., Seo, T.Y., Park, C.H., Lim, J.H., Joo, J. (2017). *Ind. Eng. Chem. Res.*, 56, 8235–8240.

[214] Edwards, J.K., Pritchard, J., Piccinini, M., Shaw, G., He, Q., Carley, A.F., Kiely, C.J., Hutchings, G.J. (2012). *J. Catal.*, 292, 227–238.

[215] Wang, Y., Yu, Y., Deng, C., Wang, J., Zhang, B.-T. (2015). *RSC Adv.*, 5, 103989–103998.

[216] Alipour, Z., Rezaei, M., Meshkani, F. (2014). *Fuel,* 129, 197–203.

[217] Parvin, T., Keerthiraj, N., Ibrahim, I.A., Phanichphant, S., Byrappa, K. (2012). *Int. J. Photoenergy.*, 2012, 1-8.

[218] López-Ramón, M.V., Álvarez, M.A., Moreno-Castilla, C., Fontecha-cámara, M.A., Yebra-Rodríguez, Á., Bailón-García, E. (2018). *J. Colloid Interface Sci.*, 511, 193–202.

[219] Chaudhuri, R.G., Paria, S., Ghosh Chaudhuri, R., Paria, S. (2012). *Chem. Rev.*, 112, 2373–2433.

[220] Zhou, C., Sun, L., Zhang, A., Wu, X., Ma, C., Su, S., Hu, S. (2015). *Chemosphere*, 125, 16–24.

[221] El-salamony, R.A. (2017). *J. Sol-Gel Sci. Technol.*, 18, 102-112.

[222] Gobara, H., El-salamony, R., Mohamed, D., Mishrif, M., *Moustafa, Y., Gendy, T. (2014).* Chem. Mater. Res., 6, 63–82.

[223] Wang, J., Liu, C., Tong, L., Li, J., Luo, R., Qi, J., Li, Y., Wang, L. (2015). *RSC Adv.*, 5, 69593–69605.

[224] Kaur, G., Singh, B., Singh, P., Kaur, M., Buttar, K.K., Singh, K., Thakur, A., Bala, R., Kumar, M., Kumar, A. (2016). *RSC Adv.*, 6, 99120–99128.

[225] Banerjee, S., Benjwal, P., Singh, M., Kar, K.K. (2018). *Appl. Surf. Sci.*, 439, 560–568.

[226] Yang, Z., Yu, A., Shan, C., Gao, G., Pan, B. (2018). *Water Res.*, 137, 37–46.

[227] Rajoriya, S., Bargole, S., George, S., Kumar, V., Gogate, P.R. (2019). *Sep. Purif. Technol.*, 209, 254–269.

[228] Kalam, A., Al-Sehemi, A.G., Assiri, M., Du, G., Ahmad, T., Ahmad, I., Pannipara, M. (2018). *Results Phys.*, 8, 1046–1053.

[229] Tyagi, M., Rana, A., Kumari, S., Jagadevan, S. (2018). *J. Clean. Prod.*, 178, 398–407.

[230] Xu, S., Zhu, H., Cao, W., Wen, Z., Wang, J., François-Xavier, C.P., Wintgens, T. (2018). *Appl. Catal. B Environ.*, 234, 223–233.

[231] Wang, Q., Liang, S., Zhang, G., Su, R., Yang, C., Xu, P., Wang, P. (2019). *Sep. Purif. Technol.*, 209, 270–278.

[232] Wang, B., Zhang, Q., Hong, J., Li, L. (2018). *Process Saf. Environ. Prot.*, 119, 75–86.

[233] Samaddar, P., Ok, Y.S., Kim, K.H., Kwon, E.E., Tsang, D.C.W. (2018). *J. Clean. Prod.*, 197, 1190–1209.

[234] Abukhadra, M.R., Rabia, M., Shaban, M., Verpoort, F. (2018). *Adv. Powder Technol.*, 29, 2501-2511.

[235] Kalapathy, U., Proctor, A., Shultz, J. (2000). *J. Chem. Technol. Biotechnol.* 468, 464–468.

[236] Yu, G., Lyu, L., Zhang, F., Yan, D., Cao, W., Hu, C. (2018). *RSC Adv.*, 8, 3312–3320.

[237] Mohamed, F., Abukhadra, M.R., Shaban, M. (2018). *Sci. Total Environ.*, 640–641, 352–363.

[238] Dong, C., Lu, J., Qiu, B., Shen, B., Xing, M., Zhang, J. (2018). *Appl. Catal. B Environ.*, 222, 146–156.

[239] Liu, N., Huang, W., Zhang, X., Tang, L., Wang, L., Wang, Y., Wu, M. (2018). *Appl. Catal. B Environ*., 221, 119–128.

[240] He, Z., Xia, D., Huang, Y., Tan, X., He, C., Hu, L., He, H., Zeng, J., Xu, W., Shu, D. (2018). *J. Hazard. Mater*., 344, 1198–1208.

[241] Gu, L., Zhu, N., Guo, H., Huang, S., Lou, Z., Yuan, H. (2013). *J. Hazard. Mater*., 246–247, 145–153.

[242] Tursi, A., Beneduci, A., Chidichimo, F., De Vietro, N., Chidichimo, G. (2018). *Chemosphere,* 201, 530–539.

[243] Zhu, F., Ma, S., Liu, T., Deng, X. (2018). *J. Clean. Prod*., 174, 184–190.

[244] Nadejde, C., Neamtu, M., Hodoroaba, V., Schneider, R.J., Paul, A., Ababei, G., Panne, U. (2015). *Applied Catal. B, Environ*., 176–177, 667–677.

[245] Rani, M., Shanker, U. (2018). *J. Colloid Interface Sci*., 530, 16–28.

[246] Chen, H., Lu, Q., He, K., Liu, M., Zhang, Y., Yao, S. (2018). *Sensors Actuators, B Chem*., 260, 908–917.

[247] Garcia, J., Gomes, H.T., Serp, P., Kalck, P., Figueiredo, J.L., Faria, J.L. (2005). *Catal. Today*, 103, 101–109.

[248] Yehia, F.Z., Eshaq, G., Rabie, A.M., Mady, A.H., Elmetwally, A.E. (2015). *Egypt. J. Pet*., 24, 13–18.

[249] Hou, X., Huang, X., Li, M., Zhang, Y., Yuan, S., Ai, Z., Zhao, J., Zhang, L. (2018). *Chem. Eng. J*., 348, 255–262.

[250] Cao, Z., Wen, X., Chen, P., Yang, F., Ou, X, Wang, S. (2018). *Colloids Surfaces A,* 549, 94–104.

[251] Moura, C.C., Helena, M., Costa, R.C.C., Fabris, D., Ardisson, D., Macedo, W.A.A., Lago, R.M. (2005). *Chemosphere*, 60, 1118–1123.

[252] Donadelli, J.A., García Einschlag, F.S., Laurenti, E., Magnacca, G., Carlos, L. (2018). *Colloids Surfaces B Biointerfaces,* 161, 654–661.

[253] Wang, J., Liu, C., Hussain, I., Li, C., Li, J., Sun, X., Shen, J., Han, W., Wang, L. (2016). *RSC Adv*., 6, 54623–54635.

[254] Cotto-Maldonado, M.C. (2012). *PhD Dissertation*. Universidad del Turabo, 1-255.

[255] Diaz, J.L., Tuesta, D., Silva, A.M.T., Faria, J.L., Gomes, H.T. (2018). *Chem. Eng. J*., 347, 963–971.

[256] An, J., Zhu, L., Wang, N., Song, Z., Yang, Z., Du, D., Tang, H. (2013). *Chem. Eng. J*., 219, 225–237.

[257] Xiong, Q., Zhou, M., Yang, H., Liu, M., Wang, T., Dong, Y., Hou, H. (2018). *ACS Sustain. Chem. Eng*., 6, 872-881.

[258] Cao, J., Xiong, Z., Lai, B. (2018). *Chem. Eng. J*., 343, 492–499.

[259] Hogland, W., Marques, M. (2016). *Chem. Eng. J*., 219, 499-511.

[260] Ozinger, N., 1997. Weitkamp (eds.): Handbook of Heterogeneous Catalysis, Wiley-VCH, Weinheim, 1-107.

[261] Rezende, C.C., Neto, J.L., Silva, A.C., Lima, V.M., Pereira, M.C., Oliveira, L.C.A. (2012). *Catal. Commun*., 26, 209–213.

[262] Jia, X., Dai, R., Sun, Y., Song, H., Wu, X. (2015). *J. Mater. Sci. Mater. Electron*., 27, 3791-3798.

[263] Casas, J.A., Rodriguez, J.J., Bautista, P., Mohedano, A.F., Mene, N. (2010). *Catal. Today*, 151, 148–152.

[264] Bansal, P., Verma, A., Talwar, S. (2018). *Chem. Eng. J*., 349, 838–848.

[265] Ma, T., Zhang, L., Xi, B., Xiong, Y., Yu, P., Li, G., Li, J., Zhao, C. (2018). *Ecol. Eng*., 110, 192–203.

[266] Sekaran, G., Karthikeyan, S., Ramani, K., Ravindran, B., Gnanamani, A., Mandal, A.B. (2011). *Environ. Chem. Lett*., 9, 499–504.

[267] Banić, N., Abramović, B., Krstić, J., Šojić, D., Lončarević, D., Cherkezova-Zheleva, Z., Guzsvány, V. (2011). *Appl. Catal. B Environ*., 107, 363–371.

[268] Cao, C.-Y., Meng, L.-K., Zhao, Y.-H. (2013). *Toxicol. Environ. Chem*., 95, 747–756.

[269] Yingcai, W., Shuai, S., Can, W., Shuai, S.F. (2018). *Environ. Prot. Eng*., 44, 132-144.

[270] May-Marrufo, A.A., Mendez-Novelo, R.I., Barceló-Quintal, I.D., Solís-Correa, H.E., Giacoman-Vallejos, G. (2017). *J. Environ. Prot. (Irvine,. Calif)*., 08, 524–539.

[271] Duarte, F., Morais, V., Maldonado-hódar, F.J., Madeira, L.M. (2013). *Chem. Eng. J*., 232, 34–41.

[272] Rostamizadeh, M., Jafarizad, A., Gharibian, S. (2018). *Sep. Purif. Technol*., 192, 340–347.

[273] Shah, J., Jan, M.R., Khitab, F. (2018). *Process Saf. Environ. Prot*., 116, 149–158.

[274] Vanamudan, A., Sadhu, M., Pamidimukkala, P.S. (2018). *J. Taiwan Inst. Chem. Eng*., 85, 74–82.

[275] Nešic, J., Manojlovic, D.D., Jovic, M., Dojcinovic, B.P., Vulic, P.J., Krstic, J., Roglic, G.M. (2014). *J. Serbian Chem. Soc*., 79, 977–991.

[276] Rashwan, W.E., Fathy, N.A., Elkhouly, S.M. (2018). *J. Taiwan Inst. Chem. Eng*., 88, 234–242.

[277] Xue, F., Yang, S.-T., Jin, X., Li, T., Wang, R., Liu, X., Bai, Y., Chen, L., Ming, Z., Yang, H. (2016). *Micro Nano Lett*., 11, 675–679.

[278] Chen, H., Motuzas, J., Martens, W., Diniz da Costa, J.C. (2018). *Sep. Purif. Technol*., 205, 293–301.

[279] Barbosa, I.A., Zanatta, L.D., Espimpolo, D.M., Silva, D.L., Nascimento, L.F., Zanardi, F.B., Filho, P.C.D.S., Serra, O.A., Iamamoto, Y. (2017). *Solid State Sci.*, 72, 14–20.

[280] Hu, L.X., Xu, D.D., Zou, L.P., Yuan, H., Hu, X. (2015). *Wuli Huaxue Xuebao/ Acta Phys. - Chim. Sin*., 31, 771–782.

[281] Molla, A., Li, Y., Khandelwal, M., Mandal, B., Kang, S.G., Hur, S.H., Chung, J.S. (2018). *J. Environ. Chem. Eng*., 6, 2616–2626.

[282] Ayodele, O.B., Lim, J.K., Hameed, B.H. (2012). *Appl. Catal*. A Gen., 413, 301-309.

[283] Wang, H., Jiang, H., Wang, S., Shi, W., He, J., Liu, H., Huang, Y. (2014). *RSC Adv.,* 4, 45809-45815.

[284] Shi, P., Su, R., Zhu, S., Zhu, M., Li, D., Xu, S. (2012). *J. hazard. Mater*., 229, 331-339.

[285] Istadi, I., Anggoro, D.D., Amin, N.A.S., Ling, D.H.W. (2011), *Bull. Chem. React. Eng. Catal*., 6 (2), 129-136.

[286] Variava, M.F., Church, T.L., Harris, A.T. (2012). *Appl. Catal. B*, 123, 200-207.

[287] Liu, T., You, H., Chen, Q. (2009). *J. Hazard. Mater*., 162, 860-865.

[288] Noorjahan, M., Kumari, V.D., Subrahmanyam, M., Panda, L. (2005). *Appl. Catal. B Env.,* 57, 291-298.

[289] Iranmahboob, J., Hill, D.O., Toghiani, H. (2001). *Appl. Surf. Sci*., 185, 72-78.